Chemical and Process Engineering Research
ISSN 2224-7467 (Paper) ISSN 2225-0913 (Online)
Vol.10, 2013
www.iiste.org

Modeling and Simulation of Temperature Profiles in a Reactive Distillation System for Esterification of Acetic Anhydride with Methanol

N.Asiedu*, D.Hildebrandt*, D.Glasser*
Centre of Material and Process Synthesis, School of Chemical and Metallurgical Engineering, University of Witwatersrand, Private mail Bag X3, Wits 2050, Johannesburg, South Africa.
*Authors to whom correspondence may be addressed:
Emails: nasiedusoe@yahoo.co.uk, Diane.Hildebrandt@wits.ac.za, David.Glasser@wits.ac.za

ABSTRACT
This paper pertains to an experimental and theoretical study of simulation of temperature profiles in a one- stage adiabatic batch distillation/reactor for the production of methyl acetate and acetic acid from the esterification of acetic anhydride with methanol. Basically it deals with the development of a mathematical model for temperature predictions in the reactor. The reaction kinetics of the process was modeled using information obtained from experimental temperature –time data during the esterification processes. The simulation results were then compared with the experimental data.
The maximum deviation of the model –predicted temperature form the corresponding experimentally measured temperature was less than 4% which is quite within the acceptable deviation range of experimental results..
Keywords: Modeling, Simulation, Reactive distillation, Temperature, Esterification, Acetic anhydride, Methanol

INTRODUCTION

The concept of reactive distillation was introduced in the 1920,s to esterification processes, Key (1932). Reactive distillation has thus become interesting alternative to conventional processes. Recently this technology has been recommended for processes of close boiling mixtures for separation. In the last years investigations of kinetics, thermodynamics for different processes have been made, Bock et al (1997), Teo and Saha (2004), Kenig at al (2001). Reactive distillation is also applied in process production of fuel ether, Mohl et al (1997). Popken (2001) studied the synthesis and hydrolysis of methyl acetate using reactive distillation technique using structured catalytic packing. The synthesis of methyl acetate has been has also been studied by Agreda et al (1990) and Kerul et al (1998). In this paper, the process considered the reactions of acetic anhydride-methanol for the production methyl acetate and acetic acid. Most of the works done on the synthesis of synthesis of methyl acetate through reactive distillation considered acetic acid and methanol reactions. This paper looks at the modeling of the kinetics of the methanol-acetic anhydride process and develops and simulates a mathematical model for the temperature-time of the reaction as the process proceed in an adiabatic batch reactor (one stage batch distillation process).

THE MATHEMATICAL MODEL OF THE REACTING SYSTEM

Given an adiabatic batch reactor the mathematical model is made up of a set of differential equations resulting from the mass and energy balances referred only to the reaction mixture because there is no heat transfer.
The stoichiometry of the reaction studied is given below:

$$(CH_3CO)_2O + CH_3OH \rightarrow 2CH_3COOH + CH_3COOCH_3$$

$$\Delta H\ (298K) = -66kJ/mol \qquad (1)$$

For a constant –volume batch reactor one can write:

$$-r_A = \frac{1}{V}\frac{dN_A}{dt} = -\frac{dC_A}{dt} \qquad (2)$$

The energy balance equation can be established as:

Heat generated = Heat absorbed by reactor contents +

Heat transferred through reactor walls (3)

$$(-\Delta H)(-r_A)Vdt + Q_{stirrer}dt = mC_p dT + UA\,(\Delta T)dt \qquad (4)$$

$$\text{Given} \quad (-r_A) = \frac{d\varepsilon}{dt} \tag{5}$$

where (ε) is the extent of reaction, we can rearrange eq(6) to give eq(8) below:

$$UA\,(\Delta T)dt + mC_p = (-\Delta H)\frac{d\varepsilon}{dt} \tag{6}$$

Assume that heat given by stirrer speed ($Q_{strirrer}$) is negligible. Integrating eq(4) gives

$$(T - T_o) + \frac{UA}{mC_p}\int_0^{\infty}(T - T_{amb})dt = \frac{(-\Delta H)}{mC_p}\Delta\varepsilon \tag{7}$$

The LSH of eq(7) can be used to correct experimental data to adiabatic conditions. It is assumed that the reaction is independent of temperature, hence correcting the experimental data the adiabatic temperature rise parameter (ΔT_{ad}) can be obtained from the experimental result for the process. This adiabatic temperature rise is equal to the RHS of eq(9) or we can write;

$$\Delta T_{ad} = \frac{(-\Delta H)\varepsilon}{mC_p} \tag{8}$$

From eq(9) one can easily show that the energy balance equation of an adiabatic batch reactor reduces to a linear form given by eq(7) as:

$$T = T_o + \Delta T_{ad}\,\varepsilon \tag{9}$$

Theoretically the adiabatic temperature rise is by definition obtained when extent of reaction (ε) =1 or conversion (x) = 1, with respect to the reactant of interest and its value can be computed in advance from the initial conditions (temperature and heat capacities) of the reacting species. Equation (9) also allows one to find extent of reaction and or conversion at any instant under adiabatic conditions by using only one measure of temperature. Then from the initial concentrations of the reactants the concentrations products can be monitored at any instant in the reactor.

THE EXPERIMENTAL SET-UP

The experimental set- up as shown in figure (6.1) below were used in all the reactions studied. The adiabatic batch reactor used in the experiments is 18/8 stainless steel thermos-flask of total volume of 500mL equipped with a removable magnetic stirrer. The flask is provided with a negative temperature coefficient thermistor connected on-line with a data-logging system. The signal from the sensor (thermistor) is fed to a measuring and a control unit amplifier and a power interface. The acquisition units are connected to a data processor. A process control engineering support data management. All physically available analog inputs and outputs as well as virtual channel are all automatically monitored and the process values are stored. The process values are transmitted in such a way that the computer screen displays profiles of voltage-time curves. Data acquisition software was used to convert the compressed data form of the history file on the hard disk into text file format. The text files are converted to excel spreadsheet and the data are then transported into matlab 2010a for analysis.

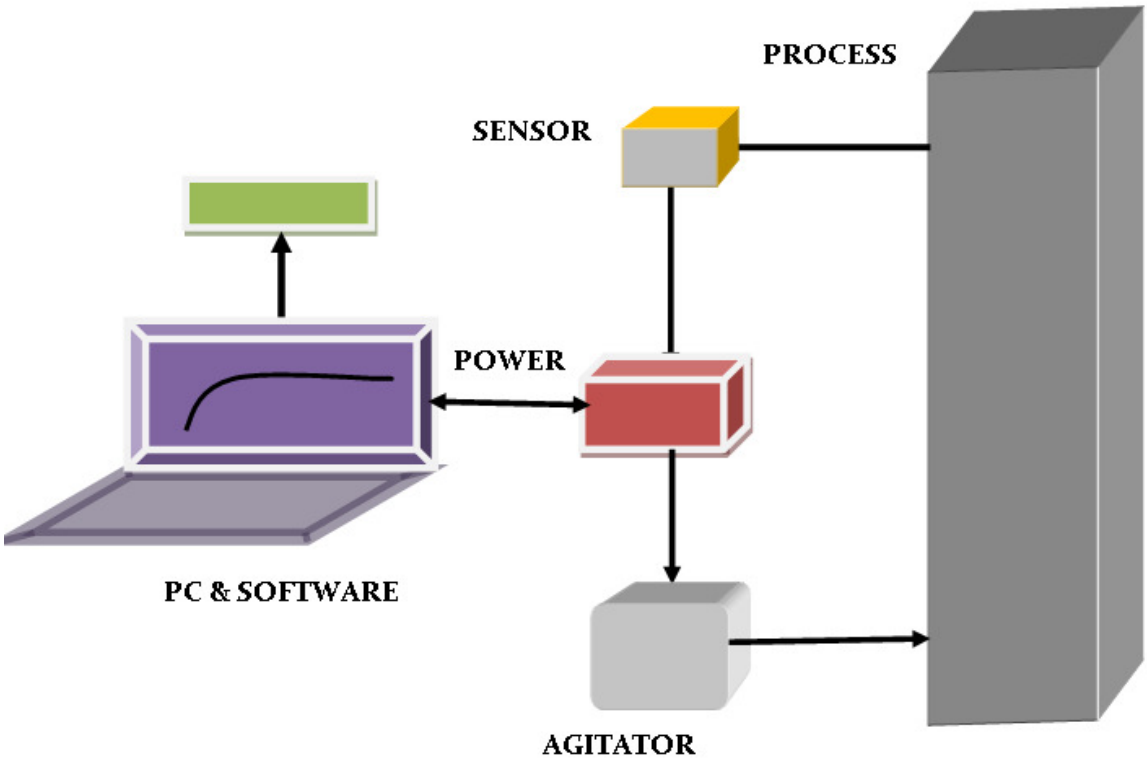

Figure (1): Block diagram of experimental set-up

THE THERMISTOR CALIBRATION

This section describes the experimental details concerning the measurements of liquid phase reactions by temperature-time techniques. Temperature changes are a common feature of almost all chemical reactions and can be easily measured by a variety of thermometric techniques.

Following the temperature changes is useful especially for fast chemical reactions where the reacting species are not easily analyzed chemically. This section thus describes the theory and the calibration of the thermistor used in the experiments described in this paper.

THE ELECRICAL CIRCUIT OF THE SYSTEM

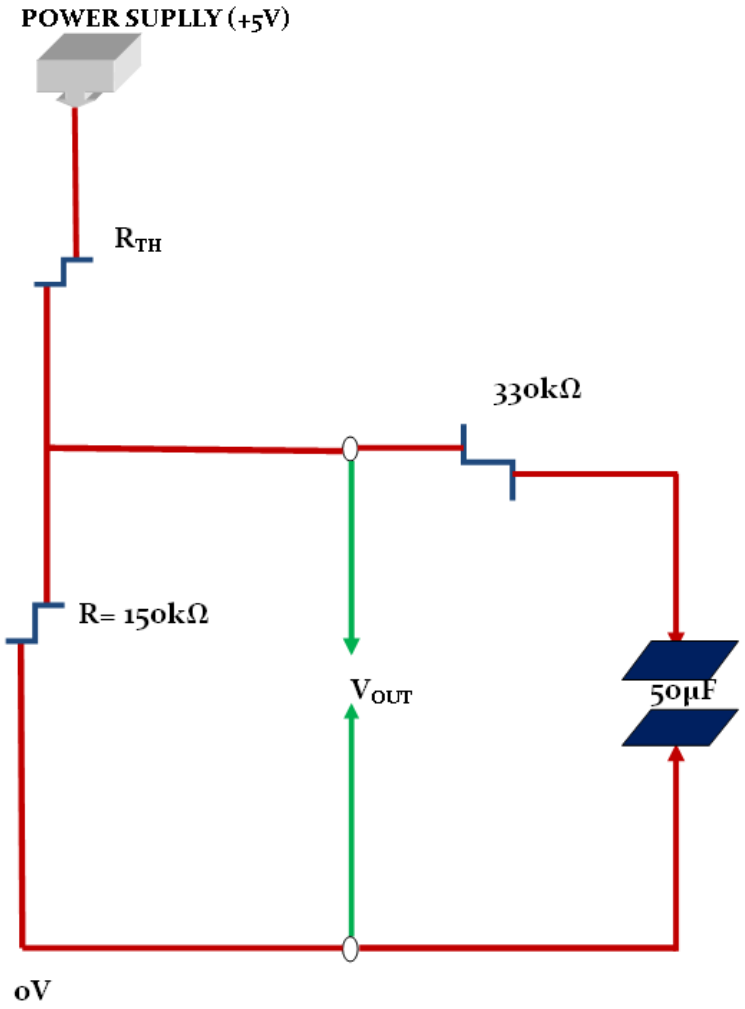

Figure(2): The electrical circuit of the system

The Circuit Theory

From Kirchhoff law's we can write:

$$V_{out} + V_{TH} = 5V \quad (10)$$

V_{out} – Voltage measured by thermistor during the course of reaction.

V_{TH} – Voltage across resistance (R_{TH}).

From (12) one can write:

$$V_{TH} = 5V - V_{out} \quad (11)$$

$$R_{TH} = \frac{V_{TH}}{I_{total}} \quad (12)$$

From the circuit V_{TH} and I_{total} are unknowns. R_{TH} is resistance due to the thermistor, and I_{total} is the same through the circuit and can be determine as :

$$I_{total} = \frac{V_{out}}{R} \quad (13)$$

V_{out} is known from experimental voltage –time profile and R (150kΩ) is also known from the circuit. Thus when I_{total} is determined from eq(13), R_{TH} which is the thermistor's resistance and related to temperature at any time during the chemical reaction can be determine as:

$$R_{TH} = \frac{V_{out}}{I_{total}} \qquad (14)$$

THE THERMISTOR CALIBRATION

The thermistor used in the experiments was negative temperature coefficient with unknown thermistor constants. The calibrations involve the determination of the thermistor constants and establish the relationship between the thermistor's resistance and temperature.

This was done by fitting both the thermistor and an electronic digital temperature measuring device in a sealed vessel and the system ws slowly warmed until the voltage reaches it asymptotic state.The thermistor was connected to a computer with data acquisition software to provide data of voltage –time real-time plot as shown in figure (3) below. The voltage –time data was used to match the temperature-time data obtained from the electronic digital temperature device.

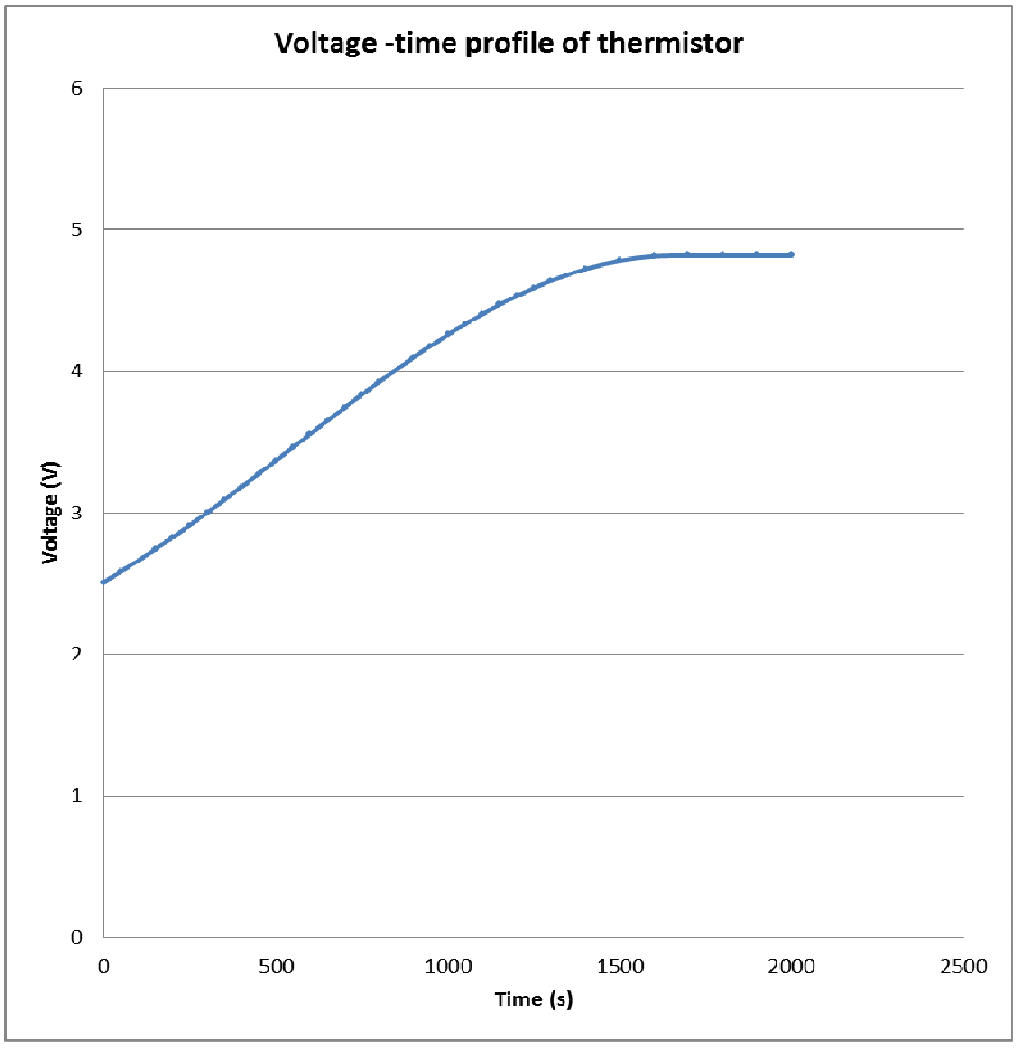

Figure(3): The thermistor voltage-time profile

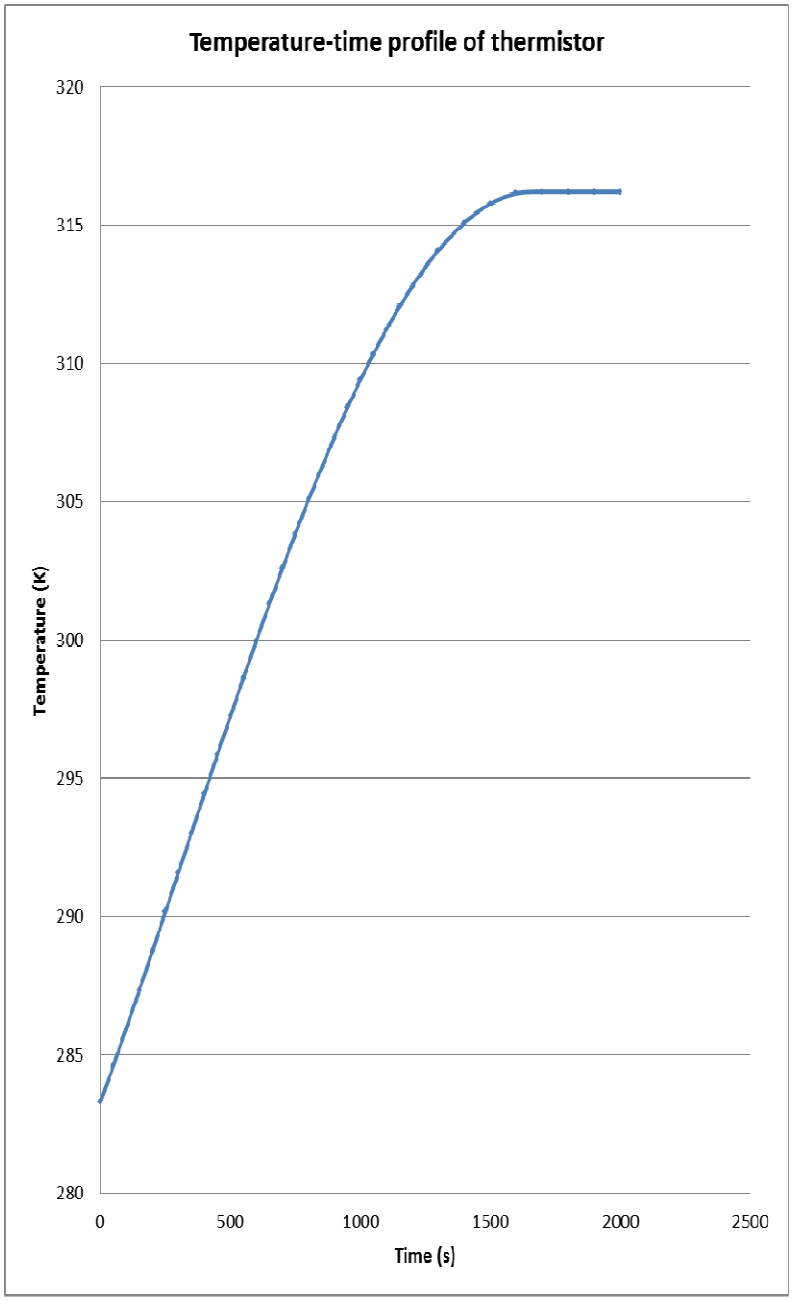

Figure(4): The thermistor temperature-time profile

RELATIONSHIP BETWEEN THERMISTOR RESISTANCE AND TEMPERATURE

Thermistor resistance (R_{TH}) and Temperature (T) in Kelvin was modeled using the empirical equation given developed by Considine (1957)

$$R_{TH} = \exp\left(\frac{B}{T} + C\right) \quad (15)$$

or

$$\ln(R_{TH}) = \frac{B}{T} + C \quad (16)$$

where the parameters (B) and (C) are the thermistor constants and were obtained from experimental calibration using warm water. The constants were determined by fitting the "best" least square straight line plot of $\ln(R_{TH})$ against 1/T, giving the thermistor equation as:

$$\ln(R_{TH}) = -\frac{1773.8}{T} + 18.178 \qquad (17)$$

The calibration plot is shown in figure (5) below:

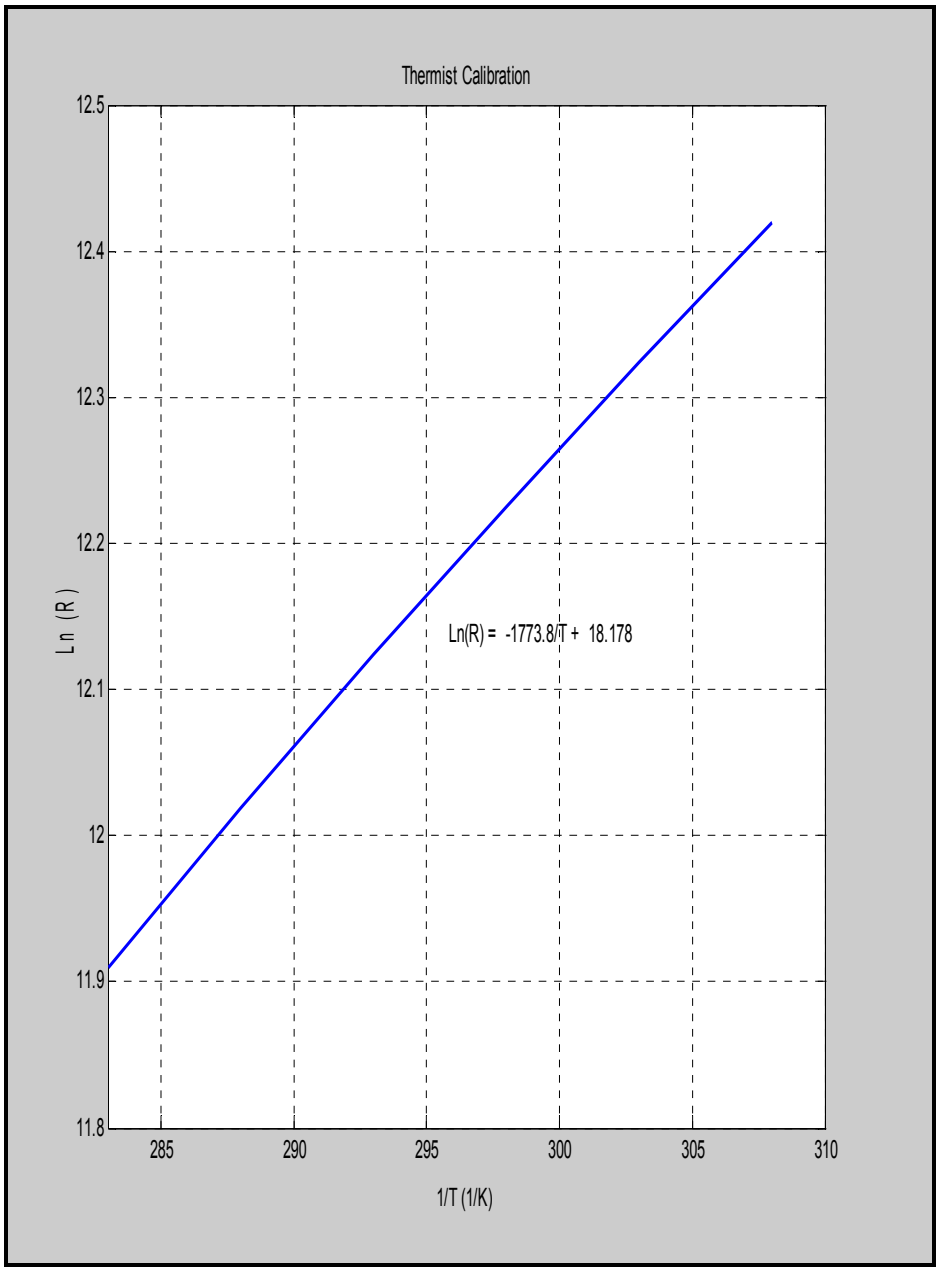

Figure(5): Regression line of $\ln(R_{TH})$ against 1/T

THE REACTOR (THERMOS-FLASK) CALIBRATION

The reaction vessel used was an ordinary dewer thermos-flask with removable screw cap lid. The flask has a total volume of 500mL. The calibration involves the determination of the heat transfer coefficient of the flask and fitting the experimental data to the model described in eq(20) below:

$$T = T_S + (T_O - T_S)\exp\left(-\frac{UA}{mC_p}t\right) \quad (18)$$

In this experiment 400.00g of distilled water at 361K (T_O) was injected into the reaction vessel and left the system temperature to fall over a period of time until the temperature-time profile reaches its asymptotic state or the steady-state temperature (T_S). The figure (6) below shows the temperature-time profile of the cooling process.

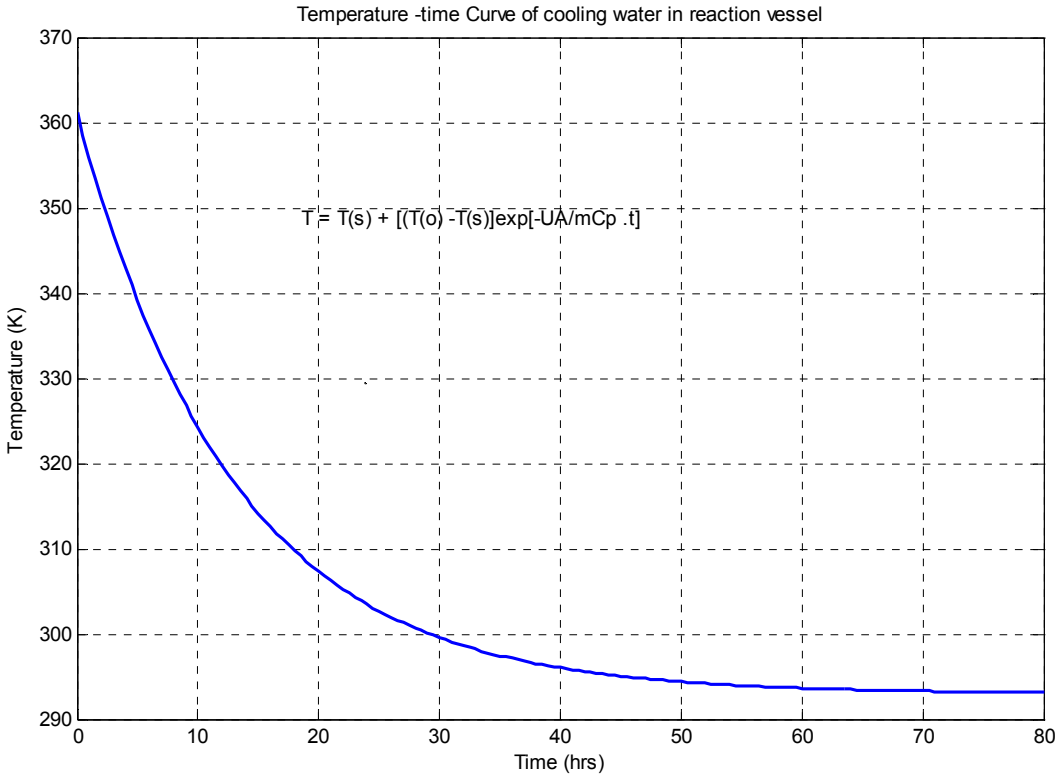

Fig (6) : Thermos-flask cooling curve at T(0) =361K

From eq(20) the values of T_o and T_s were obtained from fig(6.6). Rearrangement of eq(18) gives;

$$\ln\left(\frac{T - T_S}{T_O - T_S}\right) = \ln(\beta) = \left(-\frac{UA}{mC_p}t\right) \quad (19)$$

Since T and t values are known least square regression analysis was performed and a straight plot of ln(β) against time is shown in figure (7) below:

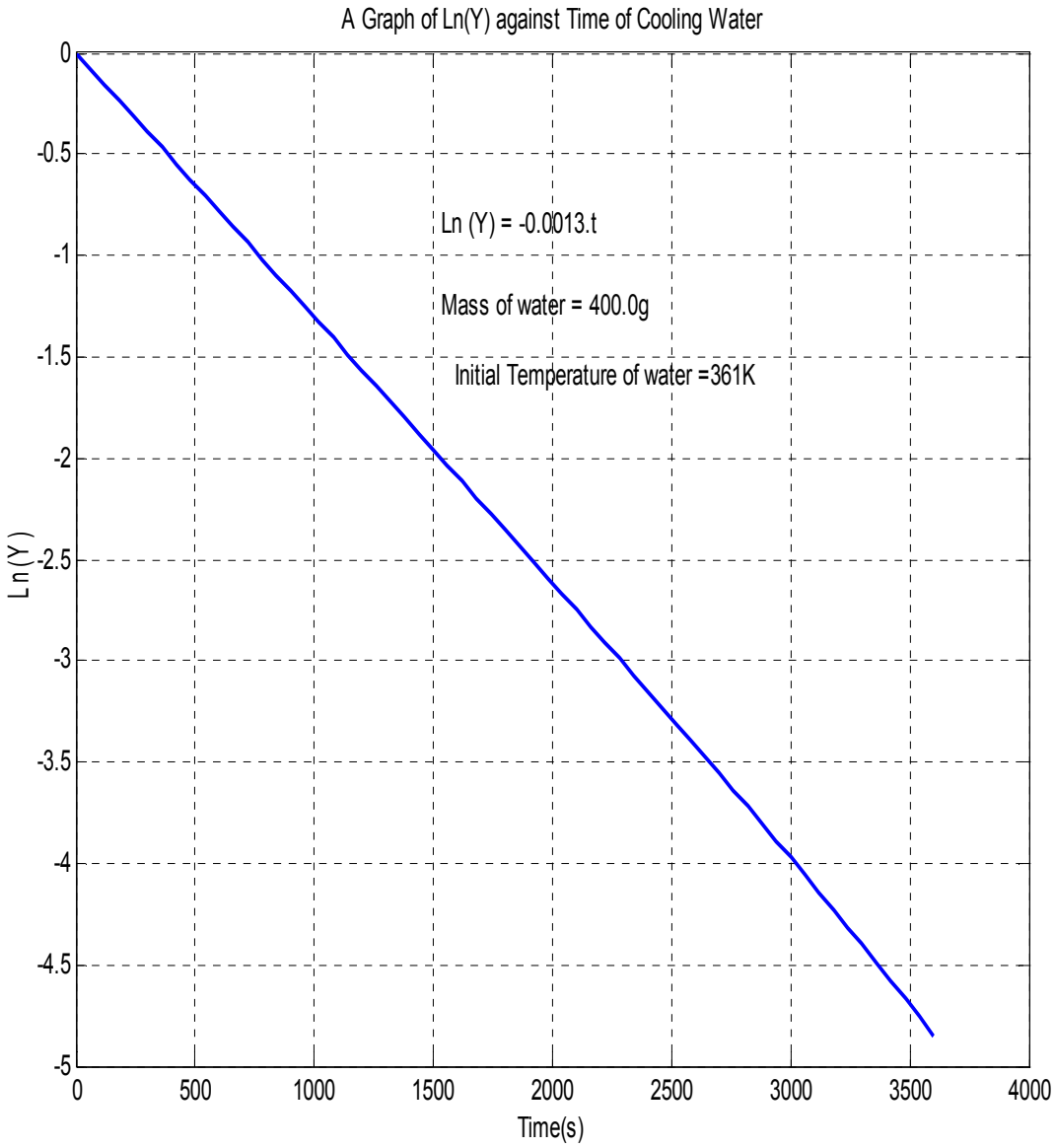

Fig (7) :Regression line of heat transfer coefficient of reactor

The slope of the straight line of fig(7) is given by $0.0013s^{-1}(min^{-1})$ which corresponds to the value of the heat transfer coefficient of the flask.

EXPERIMENTAL PROCEDURES AND RESULTS

Analytical reagent grade acetic anhydride was used in all the experiments. In all experiments about 1.0 mol of acetic anhydride was poured into the reaction vessel followed by 3.0mols of the methanol. These volumes were used so that at least 60% of the length of the sensor (thermistor) would be submerged in the resulting mixture. Reactants were brought to a steady-state temperature before starting the stirrer. In course of the reaction the stirrer speed was set 1000/ min and the resulting voltage-time profiles were captured as described above and the corresponding temperature-time curve was determined using the thermistor equation derive in equation (17) above. Runs were carried out adiabatically at the following initial temperatures: 290K, 294K and 300K.

DETERMINATION OF UA/mC$_p$ FOR THE REACTION MIXTURE

For a given system (reaction vessel and content) one can write:

$$\left(\frac{mC_p}{UA}\right)_{system} = \left(\frac{m\,C_P}{UA}\right)_{water} + \left(\frac{mC_P}{UA}\right)_{vessel} \qquad (20)$$

In this experiment different amount of water (m_w) (200g, 300g and 400g) was injected into the reaction flask at 343.08K, 347.77K and 347.85K and allowed to cool until the temperature reaches a steady-state temperature (T_S). Figures (8a), (9a) and (10a) of the cooling processes are shown below. The cooling process thus follows equation (18) above. A nonlinear least-square regression analysis was performed on all the three experimental curves. Using eq(19), the value of UA/mC$_P$ for each cooling curve was obtained. Figures (8b),(9b) and (10b) shows the regression lines.

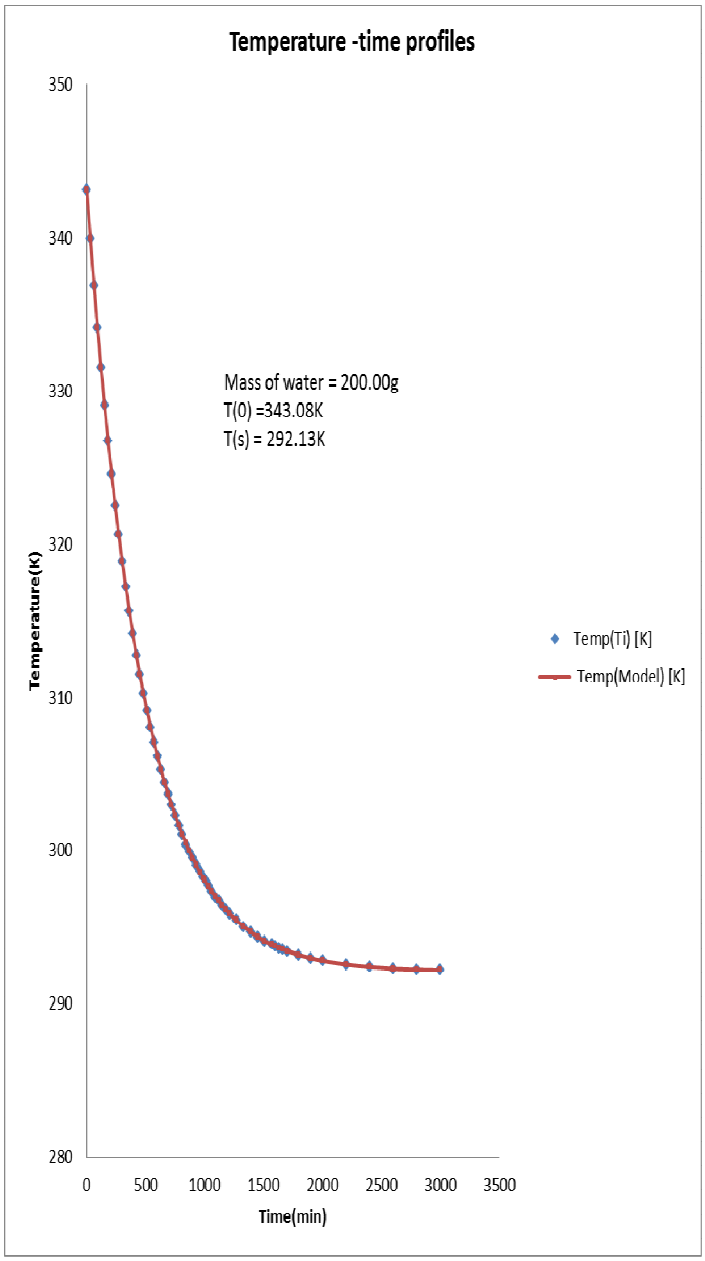

Fig (8a): Thermos-flask cooling curve at T(0) =343.08K

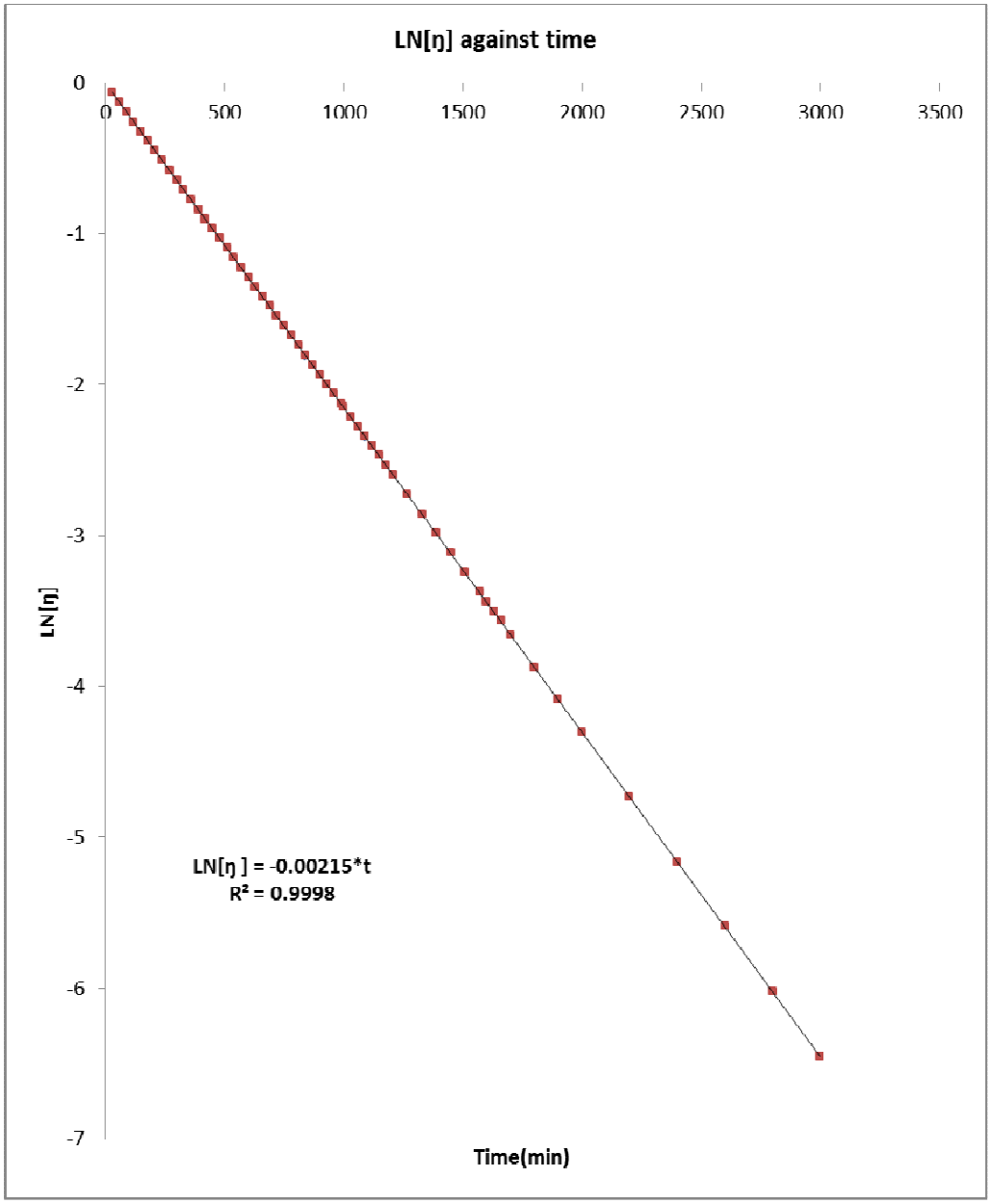

Fig (8b): Regression line of heat transfer coefficient of reactor

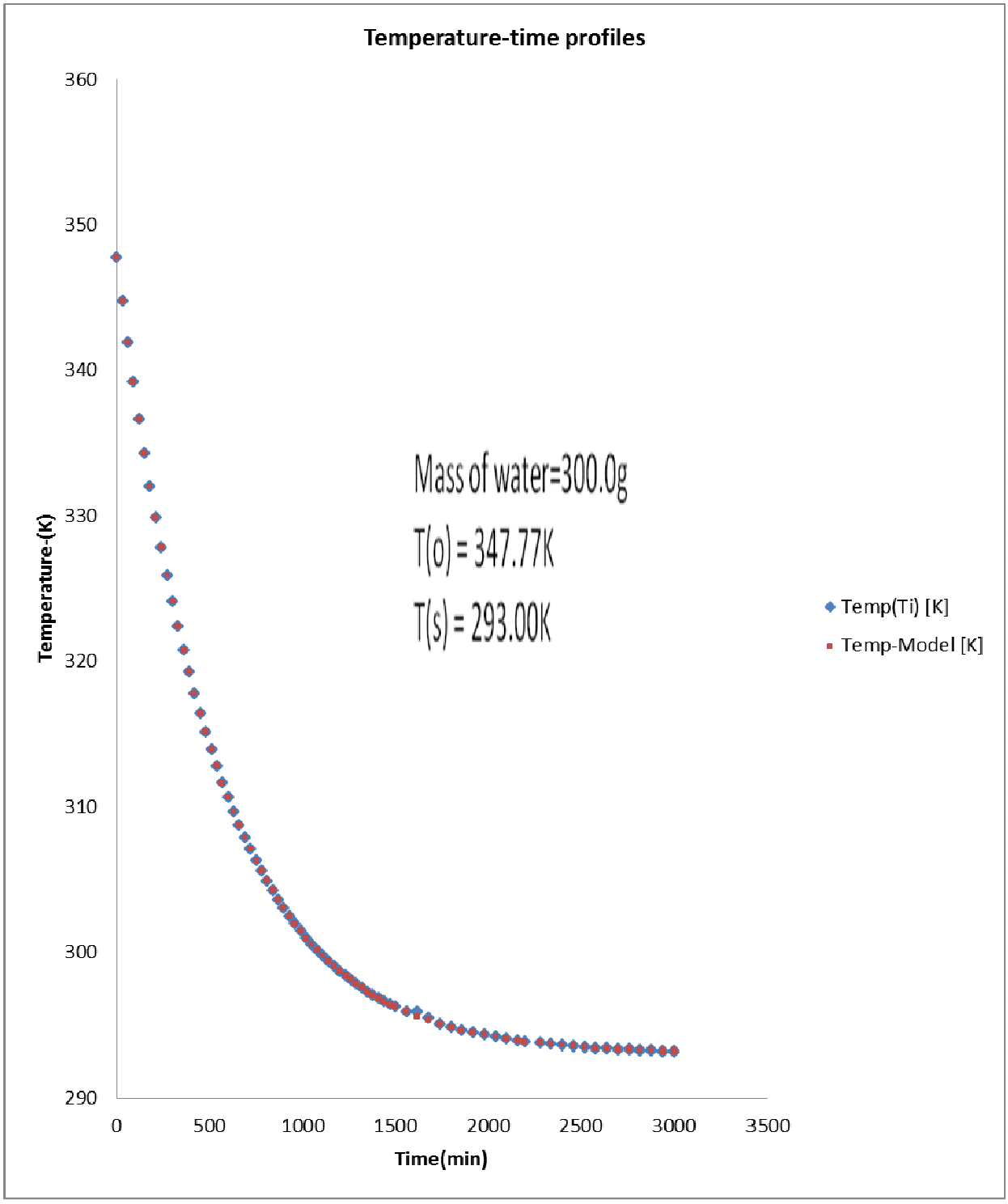

Fig (9a): Thermos-flask cooling curve at T(0) =347.77K

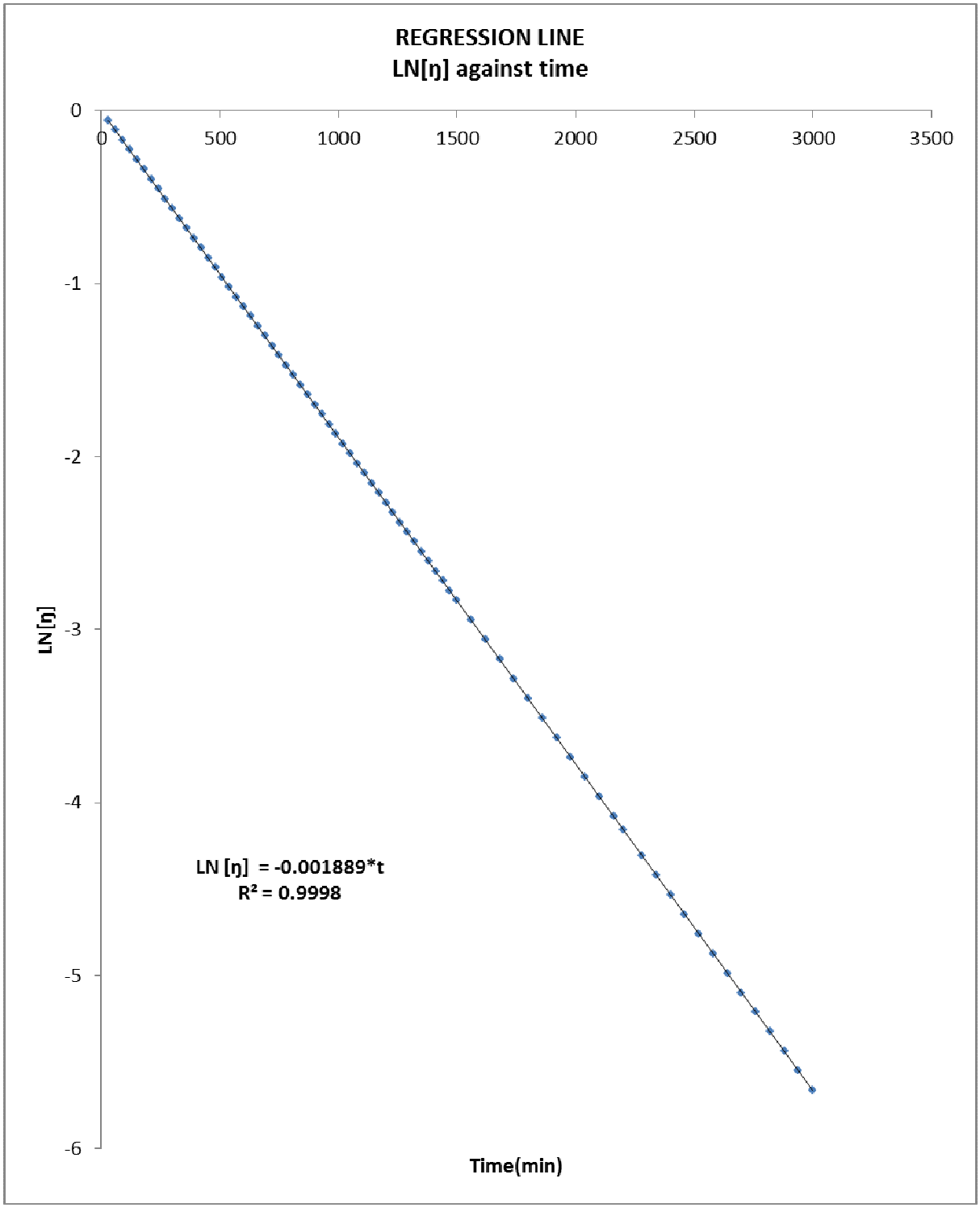

Fig (9b): Regression line of heat transfer coefficient of reactor

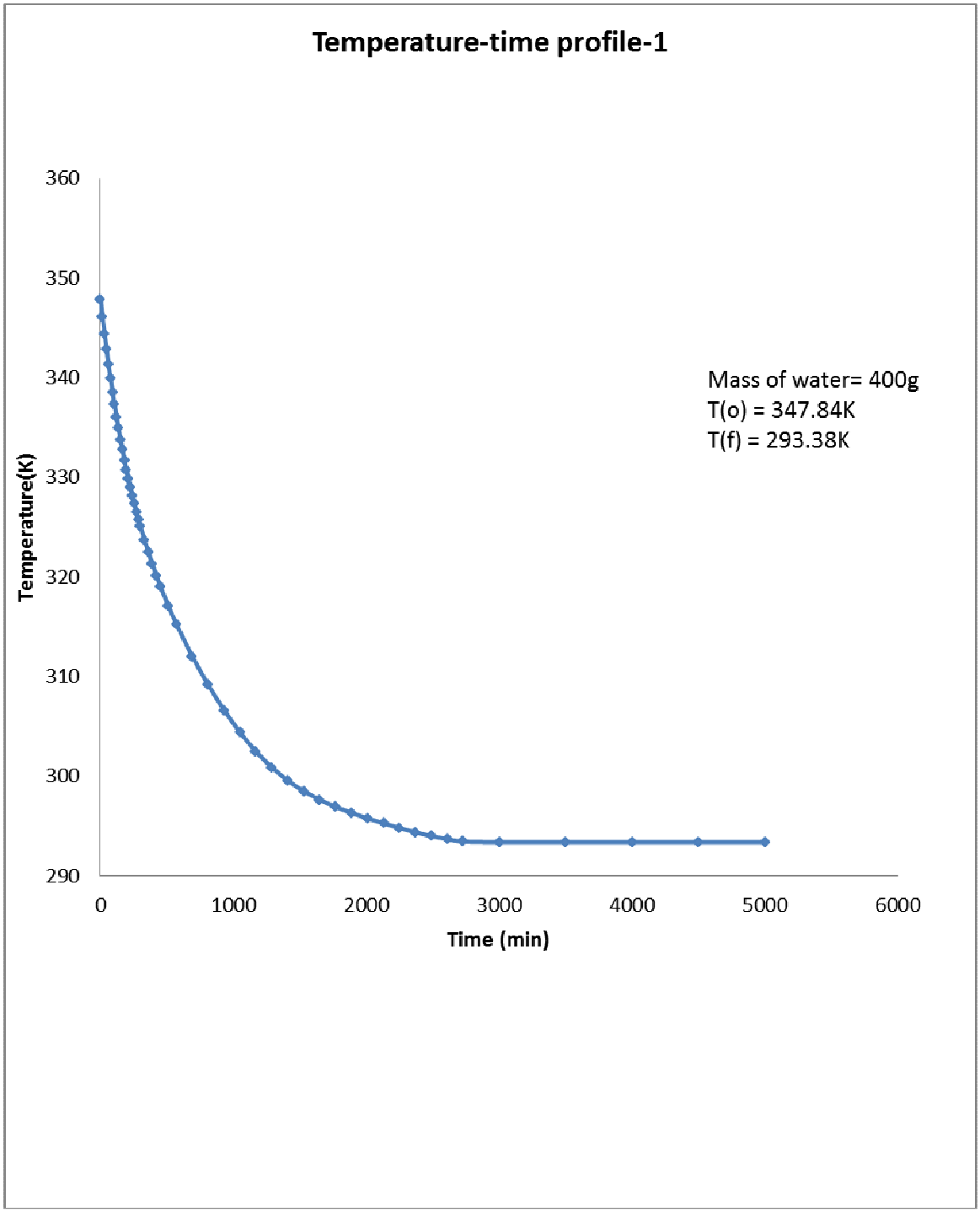

Fig (10a): Thermos-flask cooling curve at T(0) =347.80K

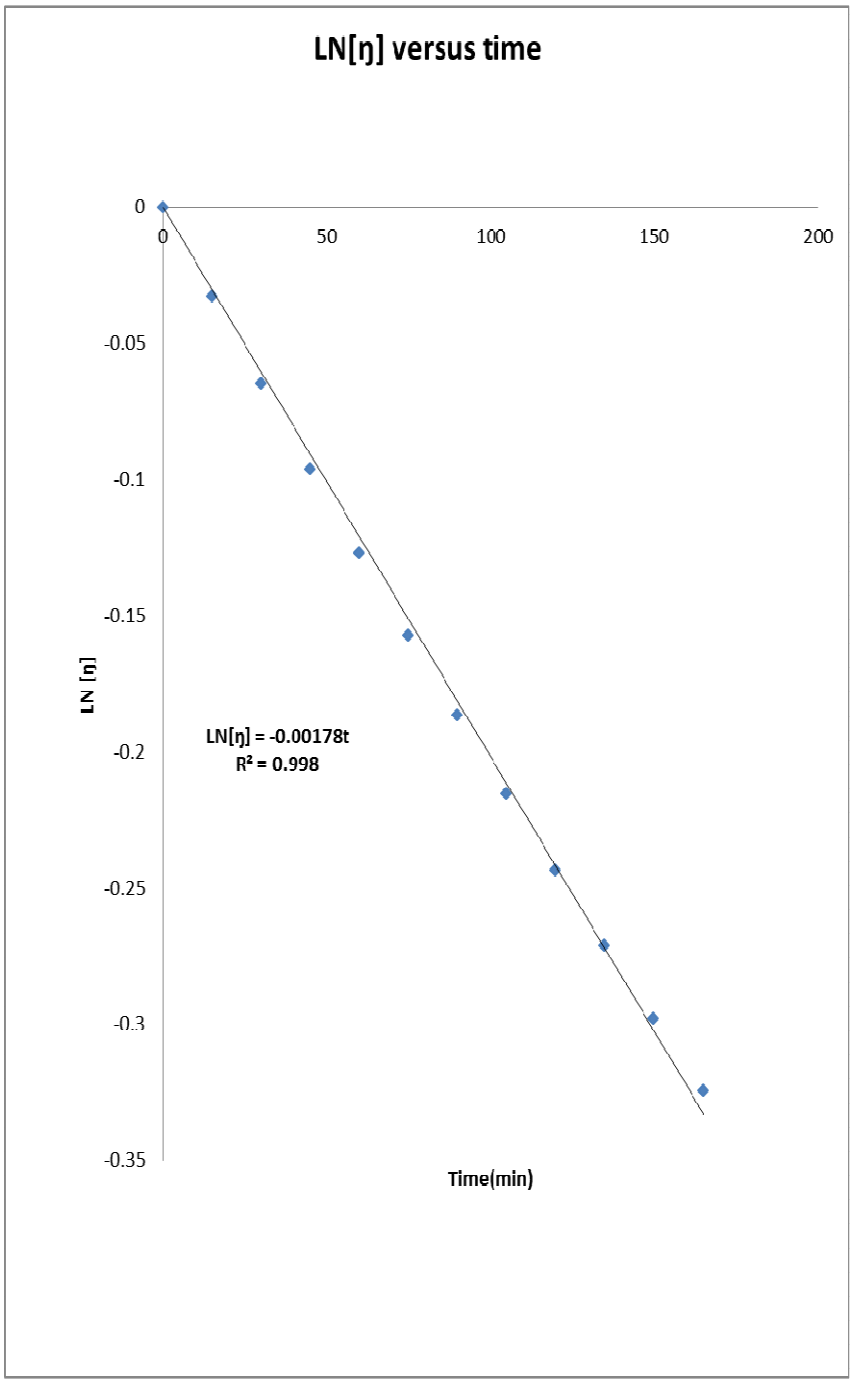

Fig (10b): Regression line of heat transfer coefficient of reactor

Table (1): Summary of characteristics of figures (6.8)-(6.10)

Mass of water(g)	Initial Temperature(K)	Final Temperature(K)	UA/mCp (min^{-1})
200	343.08	292.13	0.00215
300	347.77	293.00	0.00189
400	347.84	293.38	0.00178

From table (1) a plot of mass of water (m) against (mC_p/UA) is shown in figure(11) below:

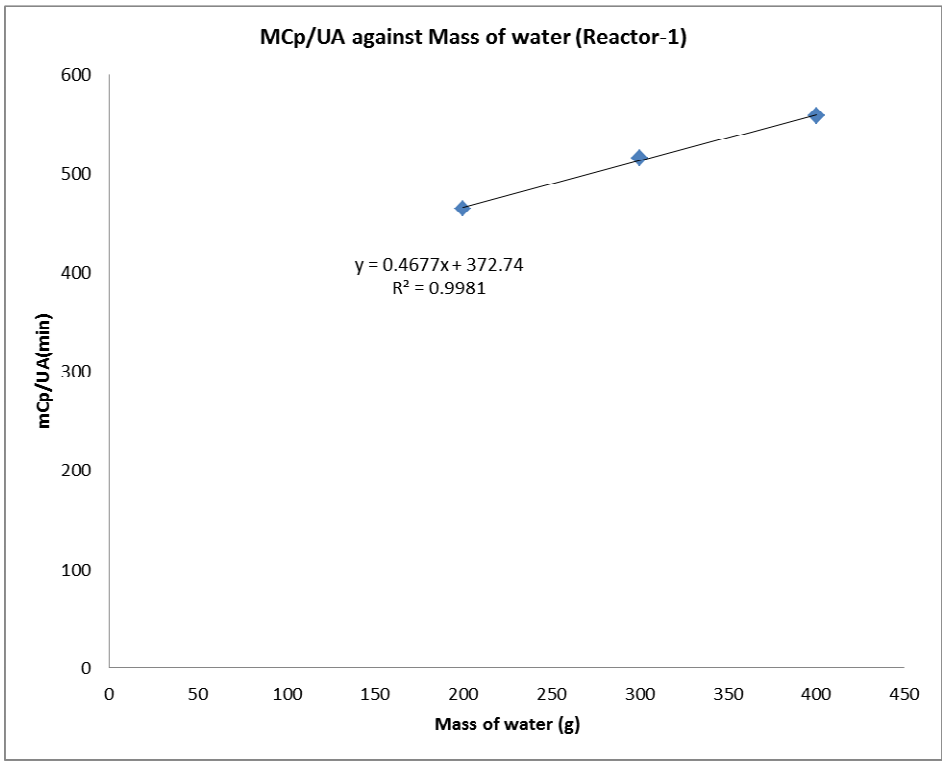

Fig (11): A plot of mass of water (m) against (mC_p/UA)

Table (2) below consist of some of the physical constants of the reacting species which was used in the determination of the quantity UA/mC_P.

Table (2) : Some constants of reacting species

Species	Moles	Molar mass(g/mol)	C_P (J/mol.K)
Acetic anhydride	1.0	102.9	189.7
methanol	3.0	32.04	79.5

Equation (21) was used to determine specific heat of the mixture ($C_{P.mix}$) and the quantity $M_TC_{P.mix}$.

$$C_{P.mix} = \frac{m_{AA}}{M_T} C_{P.AA} + \frac{m_m}{M_T} C_{P.m} \qquad (21)$$

$M_TC_{P.mix}$. was calculated to be 545.19 J/mol. K Since the reaction mixture is not pure water we therefore determined its equivalent mass of water by dividing 545.19 J/mol. K by the specific heat of water;

$$m_{eqv}\ water = \frac{(M_T\ C_P)_{mix}}{C_{P.water}} = 130.38\ g\ water \qquad (22)$$

From the equation of the line in figure (6.11) the value of the quantity $(UA/mC_P)_{mix}$ was determined to be 0.002307/min. This value was plugged in eq(7) above and the corrections of the experimental results to adiabatic conditions was performed. The figures (12),(13) and (14) below shows the experimental and the corrected temperature profiles for all the three experiments.

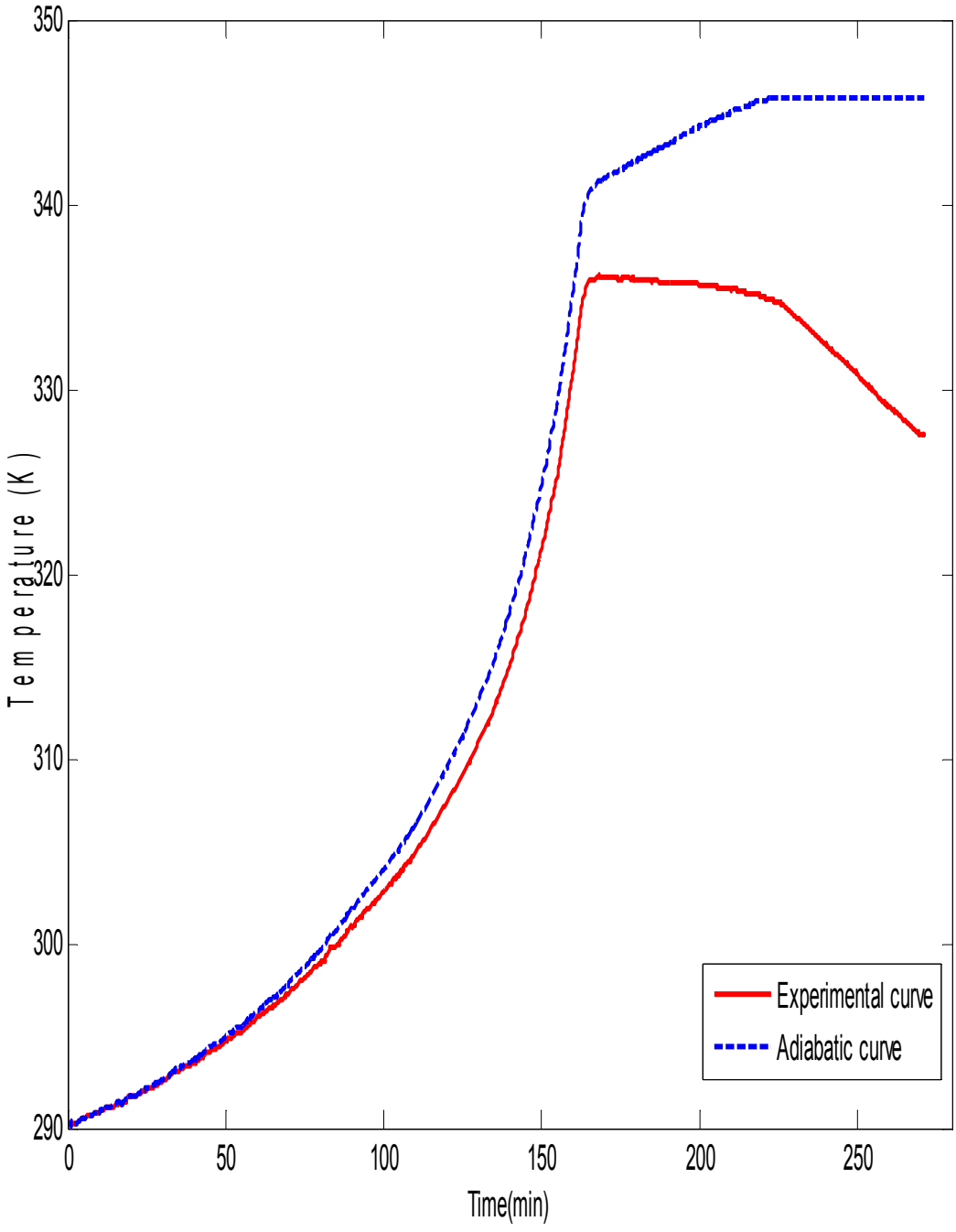

Fig(12): Experimental and Adiabatic curves of experiment-1

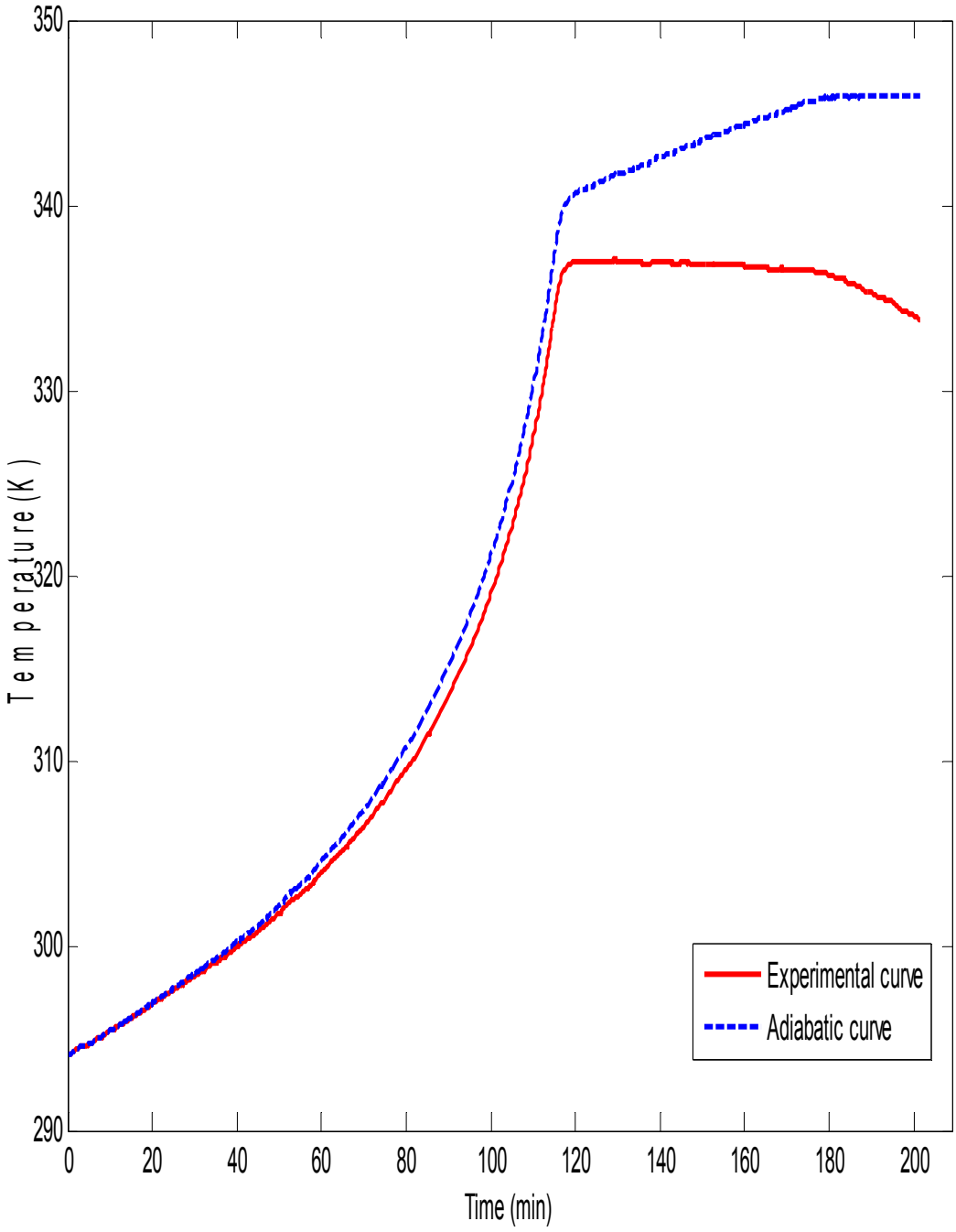

Fig(13): Experimental and Adiabatic curves of experiment-2

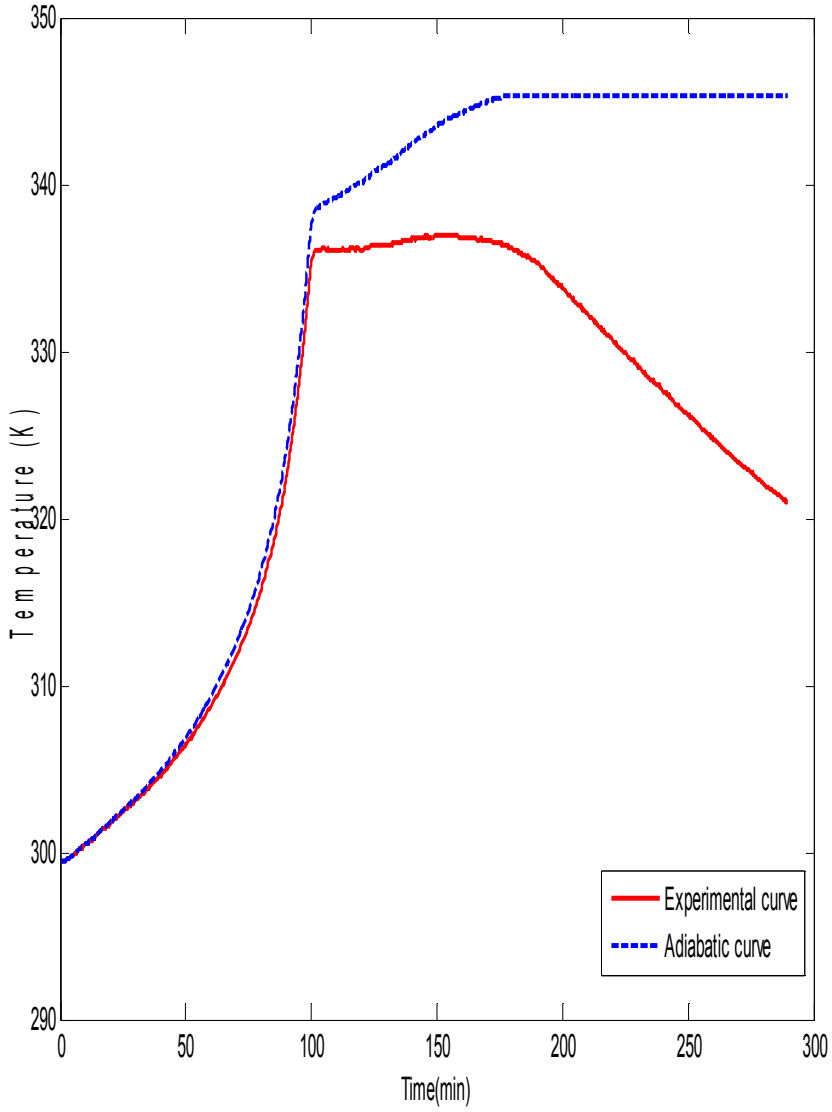

Fig(14): Experimental and Adiabatic curves of experiment-3

Table (3) : Summary of the characteristics of the above temperature-time plot

Experiment	T(0)(K)	$T_{max(adiabatic)}$(K)	$\Delta T_{exp(adiabatic)}$(K)
1	290.01	345.80	55.69
2	294.00	345.60	51.9
3	299.20	345.30	46.13

From eq(9) the variation of acetic anhydride concentration with temperature/time was deduces as:

$$C_{AA} = C_{AO} - \beta (T - T_O) \qquad (23)$$

The constant (β) in eq(23) was calculated using the initial concentration of the acetic anhydride 4.364 mol/L and the adiabatic theoretical temperature change $(\Delta T)_{adiabatic}$. The figures (15),(16) and (17) show how acetic anhydride concentration varies with time for the three experiments.

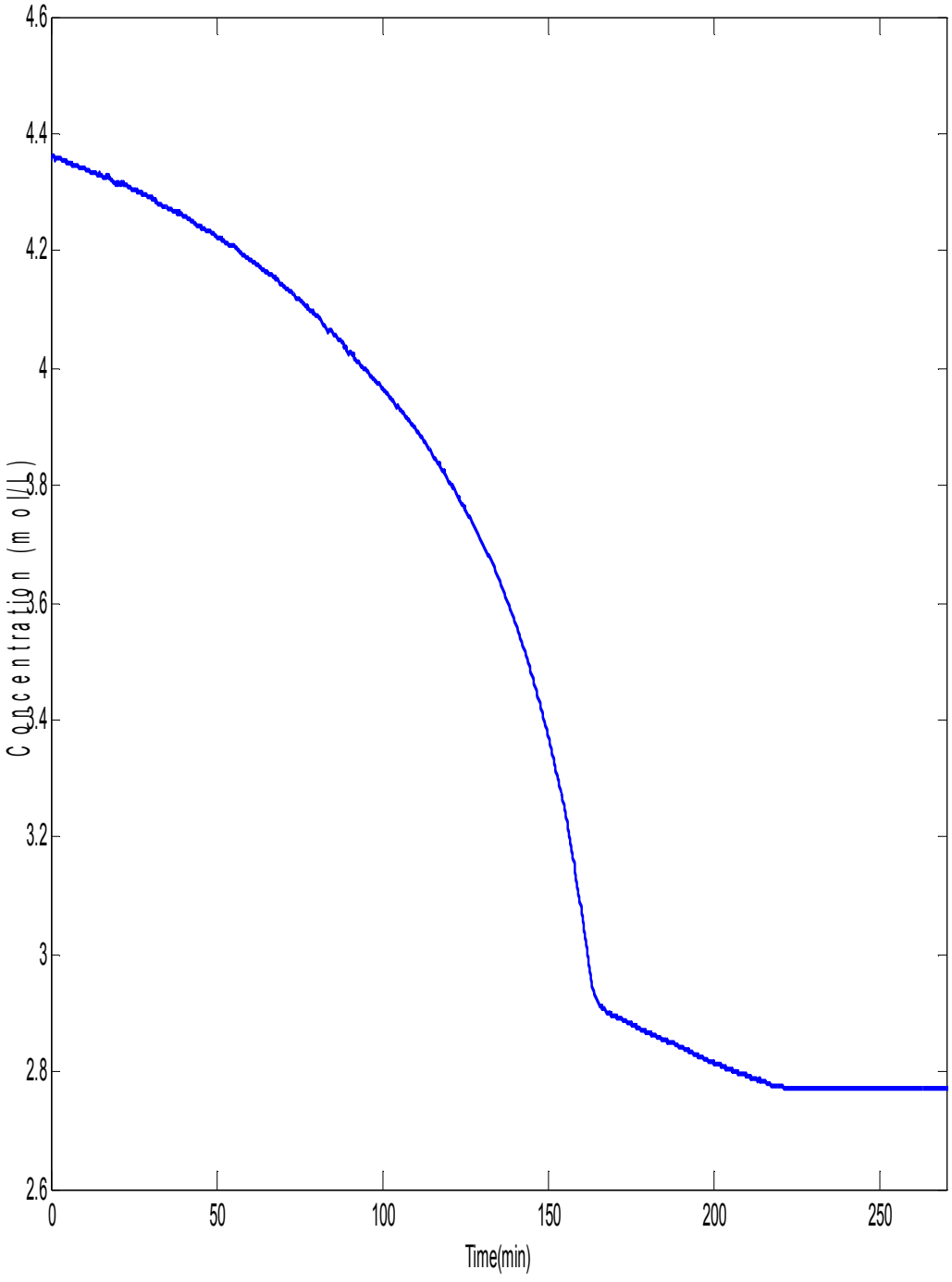

Fig (15): Concentration-time plot of acetic anhydride-Exp(1)

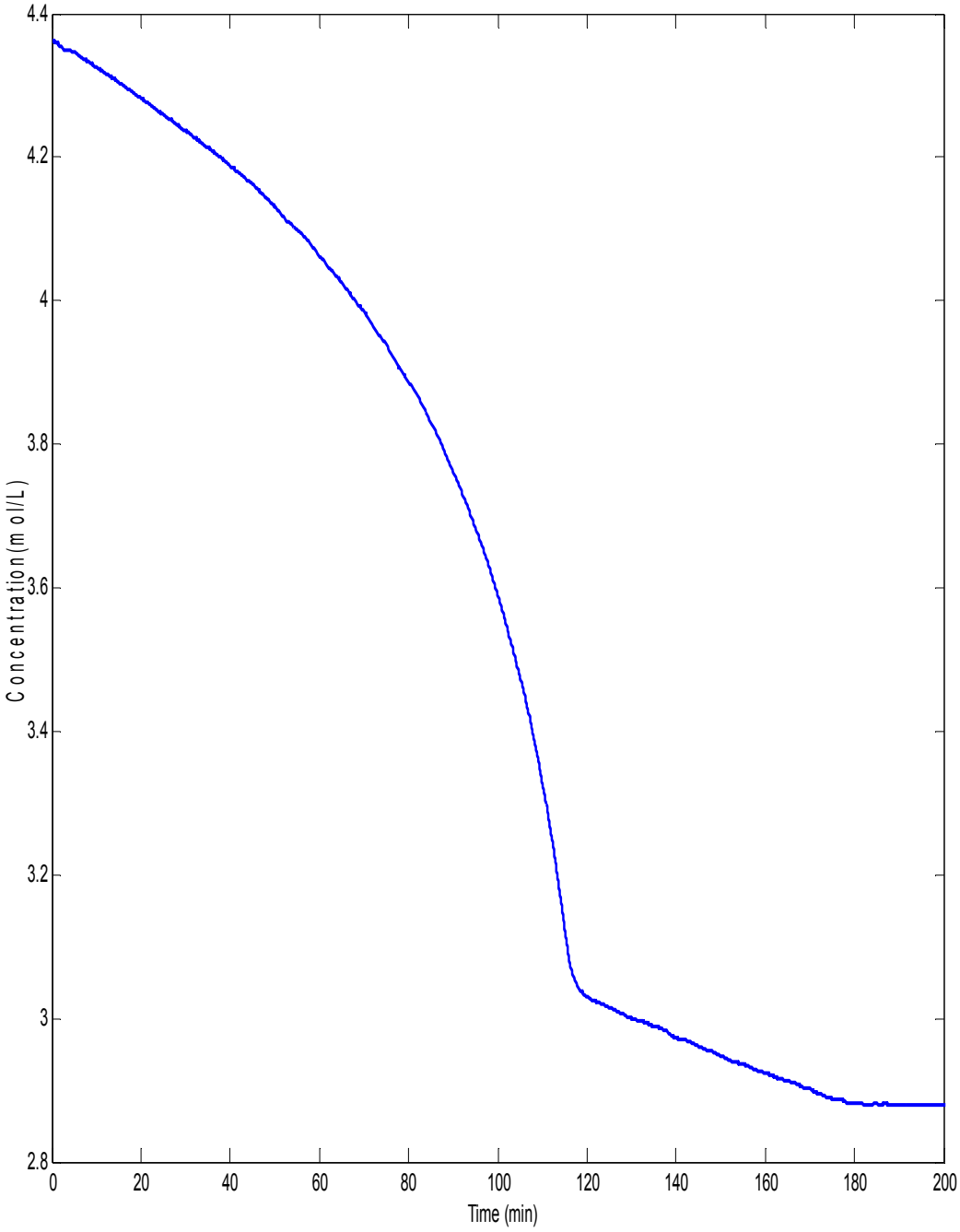

Fig (16): Concentration-time plot of acetic anhydride-Exp(2)

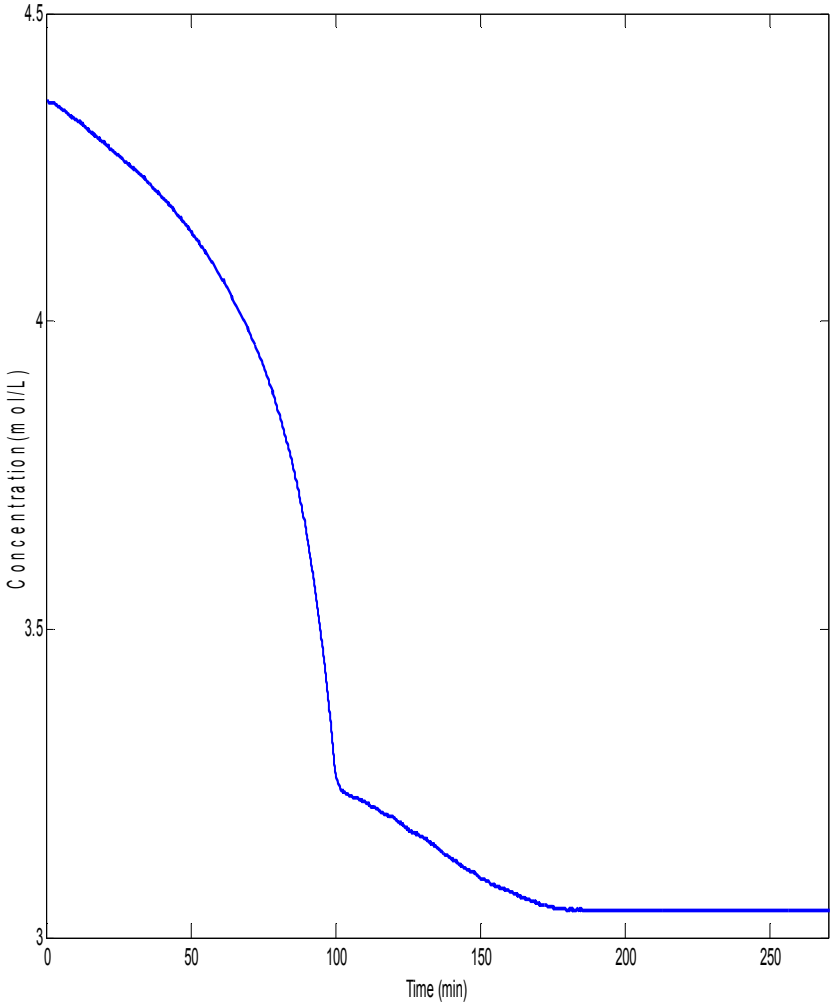

Fig (17): Concentration-time plot of acetic anhydride reaction-Exp(3)

VARIATION OF RATE VERSUS CONCENTRATION

Table (4) : Variations of temperature, rate and concentration at T =320K

	T=320K		
Experiment	Concentration	Rate	Rate constant (k)
1	3.507025023	0.03238313	0.00936158
2	3.620338071	0.033438511	0.00923629
3	3.765872632	0.03500009	0.00929425
Average (k)		0.00936158	
Standard deviation (k)		6.27008E-05	

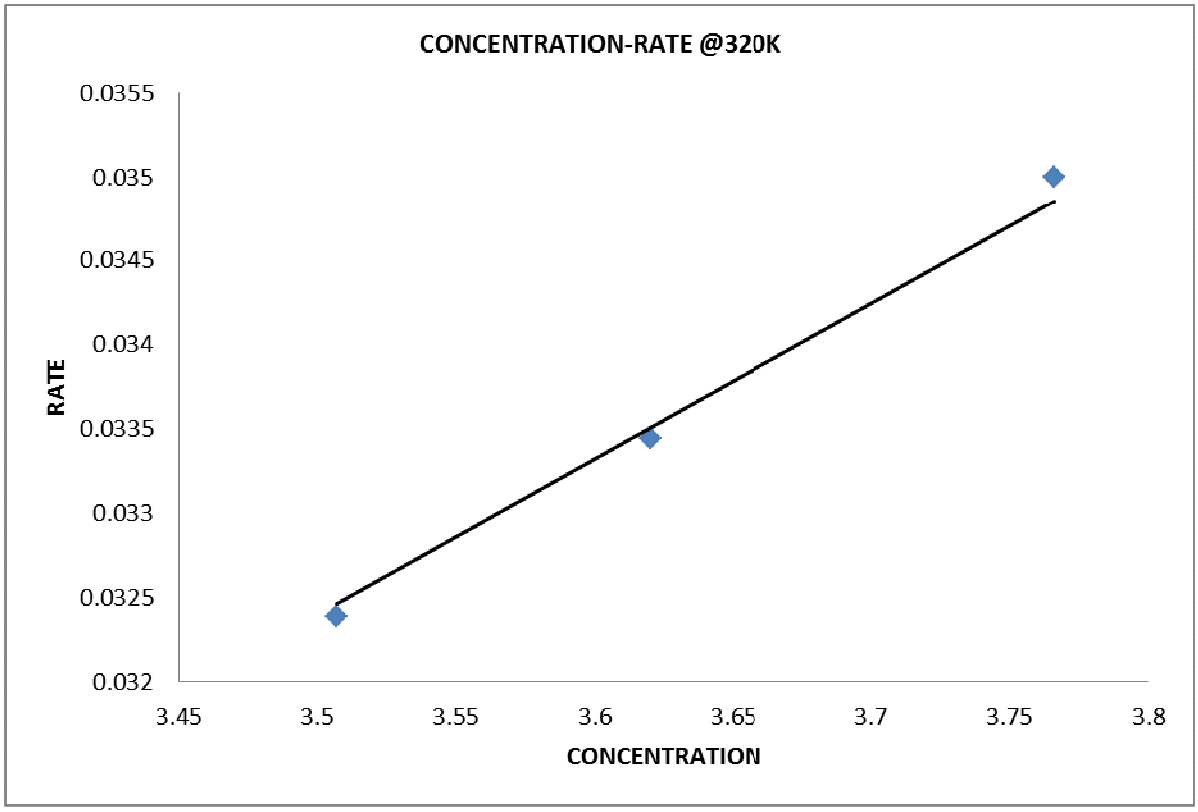

Figure(18): Concentration-rate plot @ T=320K

Table (5) : Variations of temperature, rate and concentration at T =325K

	T=325K		
Experiment	Concentration	Rate	Rate constant (k)
1	3.363932095	0.025762791	0.007658535
2	3.476755343	0.027443908	0.00789354
3	3.625365284	0.030256856	0.008345878
Average (k)		0.007965984	
Standard deviation (k)		0.000349351	

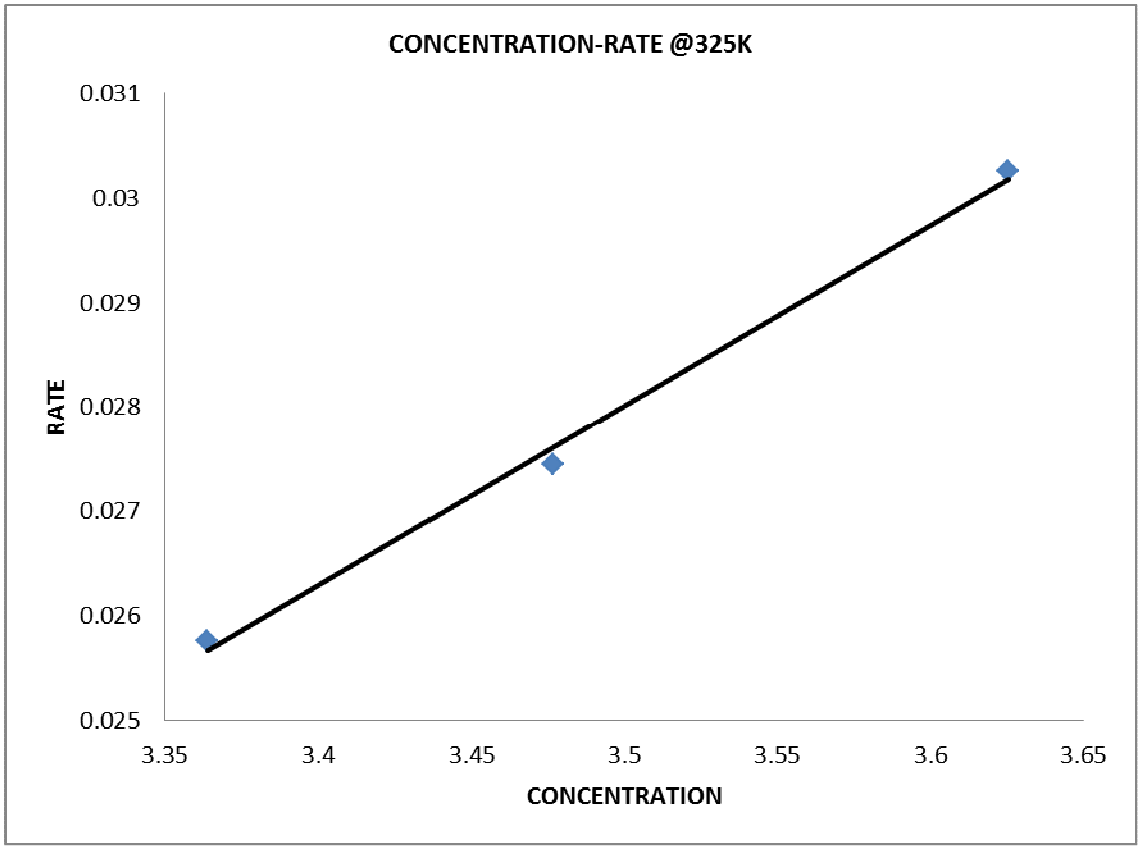

Figure(19): Concentration-rate plot @ 325K

Table (6) : Variations of temperature, rate and concentration at T =335K

	T=335K		
Experiment	Concentration	Rate	Rate constant (k)
1	3.077605537	0.041685326	0.013544727
2	3.186062023	0.04299617	0.013495082
3	3.339671258	0.045253824	0.013550382
Average (k)		0.013530064	
Standard deviation (k)		3.04267E-05	

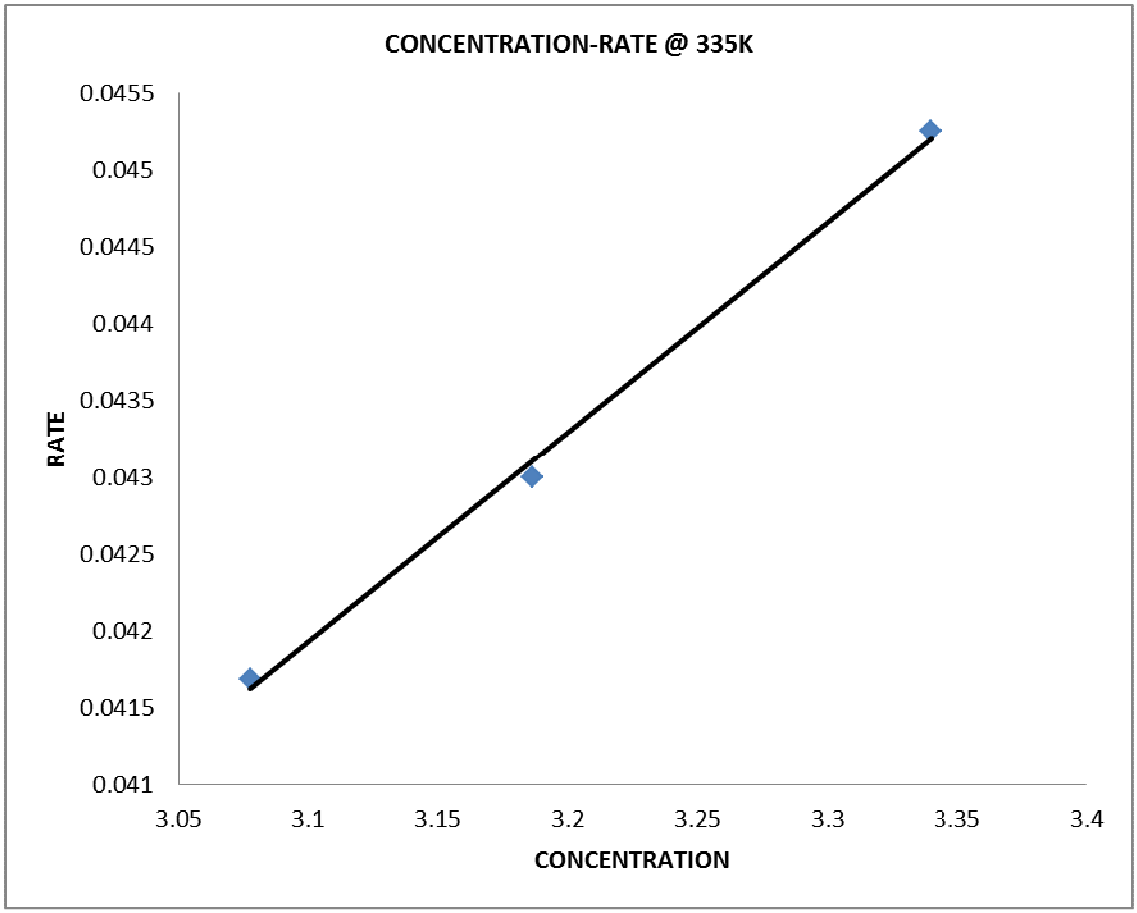

Figure(20): Concentration-rate plot @ 335K

KINETICS AND THERMODYNAMIC ANALYSIS OF THE EXPERIMENTS

The rate information obtained from the concentration-time plot enabled one to calculated specific rate constant k(T) of the processes at any time (t) and temperature (T).

Arrhenius plots was thus generated from which kinetic parameters of the runs was extracted. The figures (21), (22) and (23) below show the Arrhenius plots for all the three experiments.

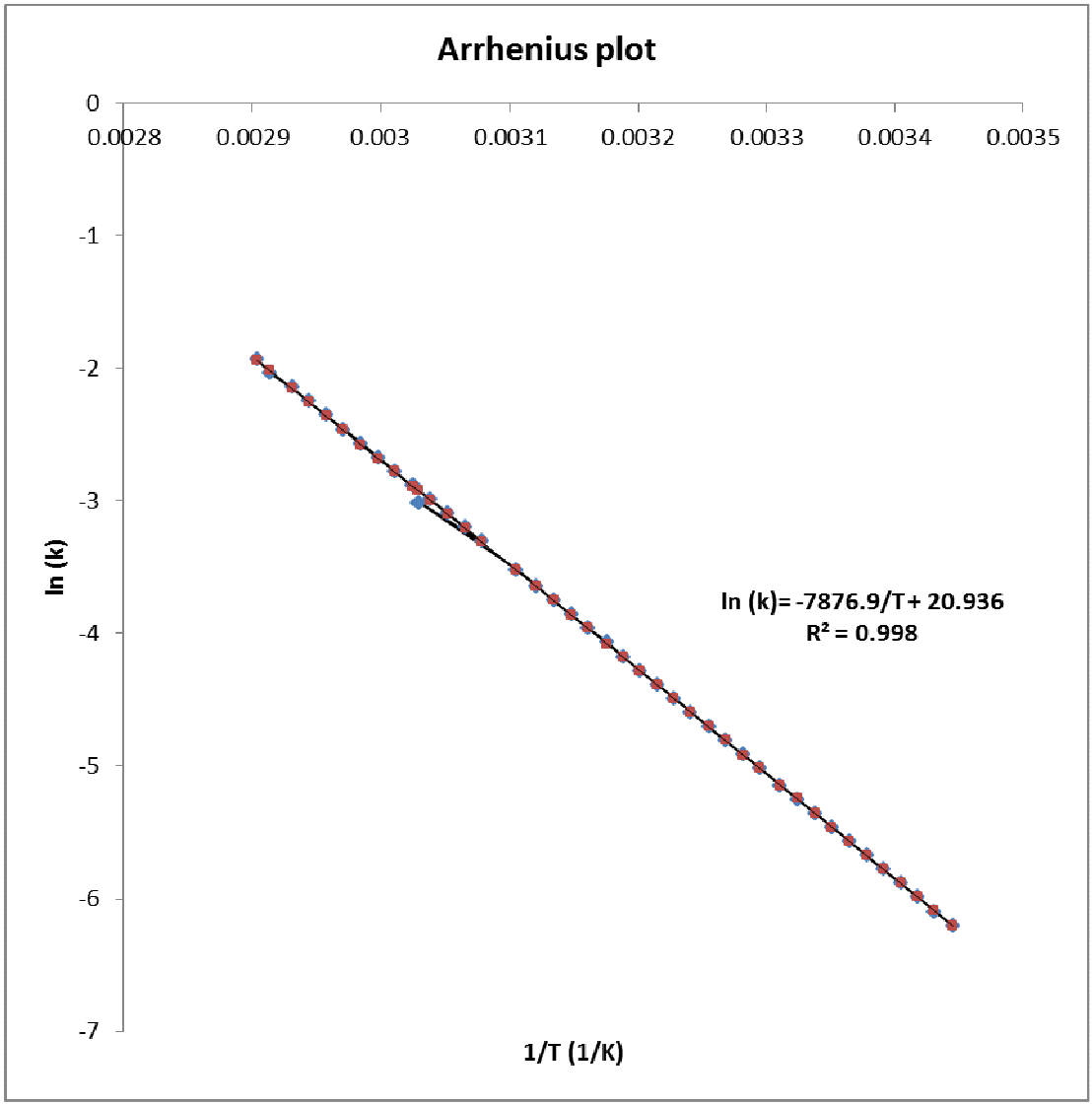

Figure (21): Arrhenius plot of experiment-1

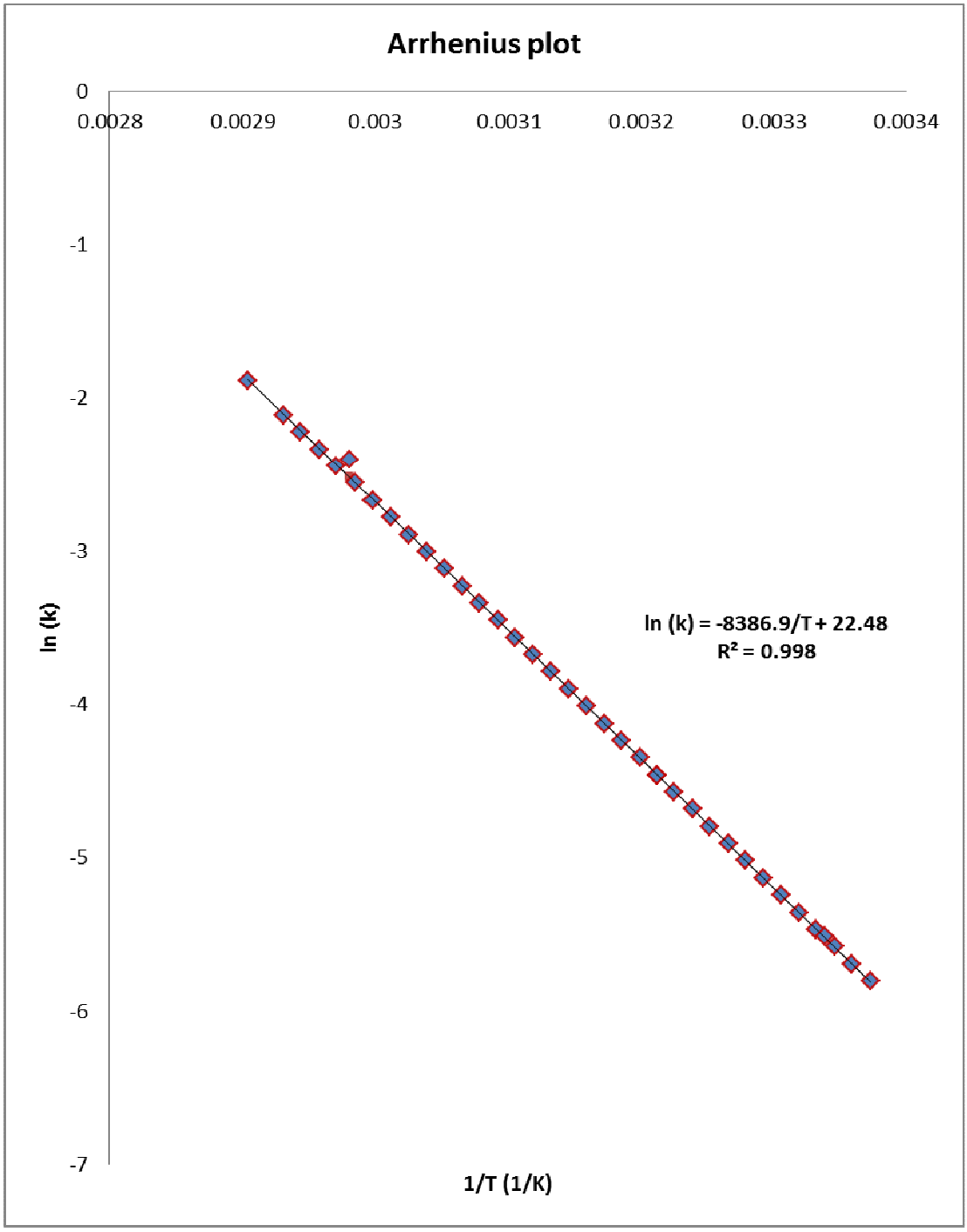

Figure (22): Arrhenius plot of experiment-2

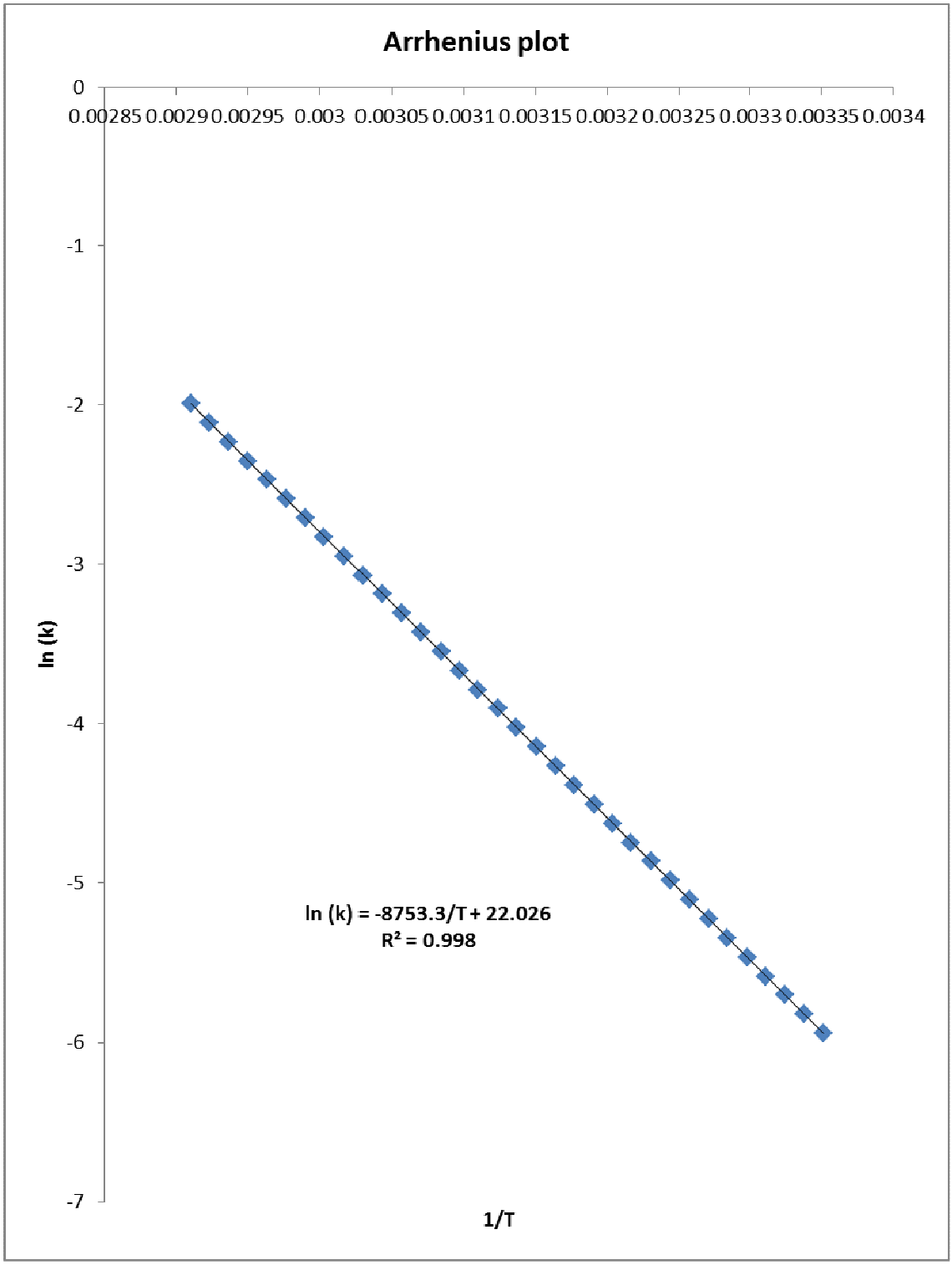

Figure (23): Arrhenius plot of experiment-3

The values obtained for the specific rate constants as a function of temperature are given in equations (24),(25) and (26) below:

$$k_1(T) = 1.24 * 10^9 exp\left(-\frac{65.49}{RT}\right) \quad (24)$$

$$k_2(T) = 5.79 * 10^9 exp\left(-\frac{69.78}{RT}\right) \quad (25)$$

$$k_3(T) = 3.68 * 10^9 \exp\left(-\frac{72.77}{RT}\right) \quad (26)$$

The thermodynamic information extracted from the experiments was the heat of the reaction (ΔH_{rxn}). This was assumed to be independent of temperature and was determined by using eq(10). Table(7) below shows ΔH_r values of the various experiments.

Table (7): Thermodynamic information of the experiments

Experiment	1	2	3
ΔH_{rxn}(kJ/mol)	61.59	61.58	61.58

MODELING APPROACH

The experimental work discussed has shown that the reactions between the acetic anhydride and methanol occurring in adiabatic batch reactor (thermos-flask) exhibit a first order reaction kinetics with respect to the acetic anhydride. This is discussed in the section 6.8 above. The kinetic parameters of the reactions are discussed in section 6.9 above. Thus for a first order adiabatic batch process, one can write design equation, rate law expression and stiochiometry equations describing the process are as follow:

a) Design Equation:

$$N_{A0}\frac{dX}{dt} = -r_A V \quad (27)$$

b) Rate law:

$$-r_A\, k(T) C_A \quad (28)$$

c) Stiochiometry:

$$C_A = \left(\frac{N_{A0}}{V}\right)(1 - X) \quad (29)$$

It assumed that since there is negligible or no change in density during the course of the reaction, the total volume **(V)** is considered to be constant. Combining equations (27) –(29), a differential equation describing the rate of change of conversion (X) with respect to time can be written as:

$$\frac{dX}{dt} = k(T)(1 - X) \quad (30)$$

$$\text{where } k(T) = A * \exp\left(-\frac{E_A}{RT}\right) \quad (31)$$

The kinetic parameters, pre-exponential constant (A) and the activation energy (E_A) has been determined experimentally in all the three reactions as discussed in section 6.9 above. The adiabat of the processes can be written as:

$$T = T_0 + \Delta T_a * X \quad (32)$$

Differentiating equation (32) with respect to time and plugging in equation (30) gives equation (33):

$$\frac{dT}{dt} = k(T) * \{[T_0 + \Delta T_a] - T\} \quad (33)$$

$$\text{where } k(T) = A * \exp(-\frac{E_A}{RT}) \quad (34)$$

For a given process, given T_o, ΔT_a, A and E_a as initial starting points, simultaneous solution of equations (33) and (34) with the help of Matlab (R2010a) program was used in the simulations process.

MODEL VALIDATION

The formulated models were validated by direct analysis and comparison of the model –predicted temperature (T) and the values obtained from experimental measurements for equality. Analysis and the comparison between the model predicted temperature values and the experimentally measured temperature values show some amount of deviation of the model-predicted temperature values from the experimentally measured values. The deviation in model equations results may be due to non-incorporation of some practical conditions in the model equation and solution strategy. Also assumptions made in the model equation's development may be responsible in the deviation of the model results. This can be improved by refining the model equation, and introduction of correction factor to the bring model- predicted temperature values to those of the experimental values.Percentage deviation (% D_{model}) of model-predicted temperature from experimentally measured values is given by equation (35) below:

$$D_{model}(\alpha) = \left(\frac{M - E}{E}\right) * 100\ \% \qquad (35)$$

where the correction factor (β) = -(D_{model}) (36)

and (M)-model-predicted temperature, and (E)-experimentally measured temperature.

The model is also validated by considering the correlation coefficients (R^2) of the model-predicted temperature and the experimentally measured temperature.

RESULTS

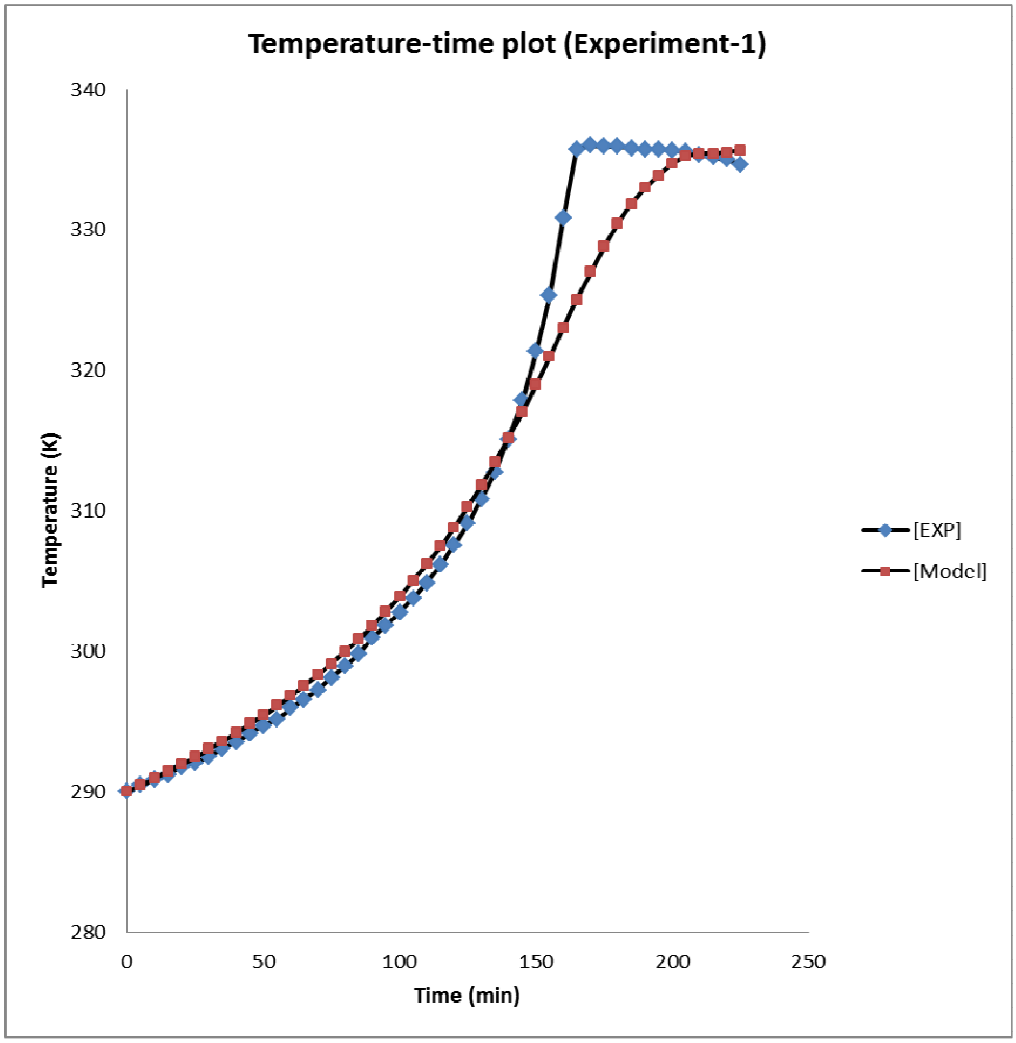

Figure (24a): Comparison of the model- predicted and experimentally measured temperature for experiment (1)

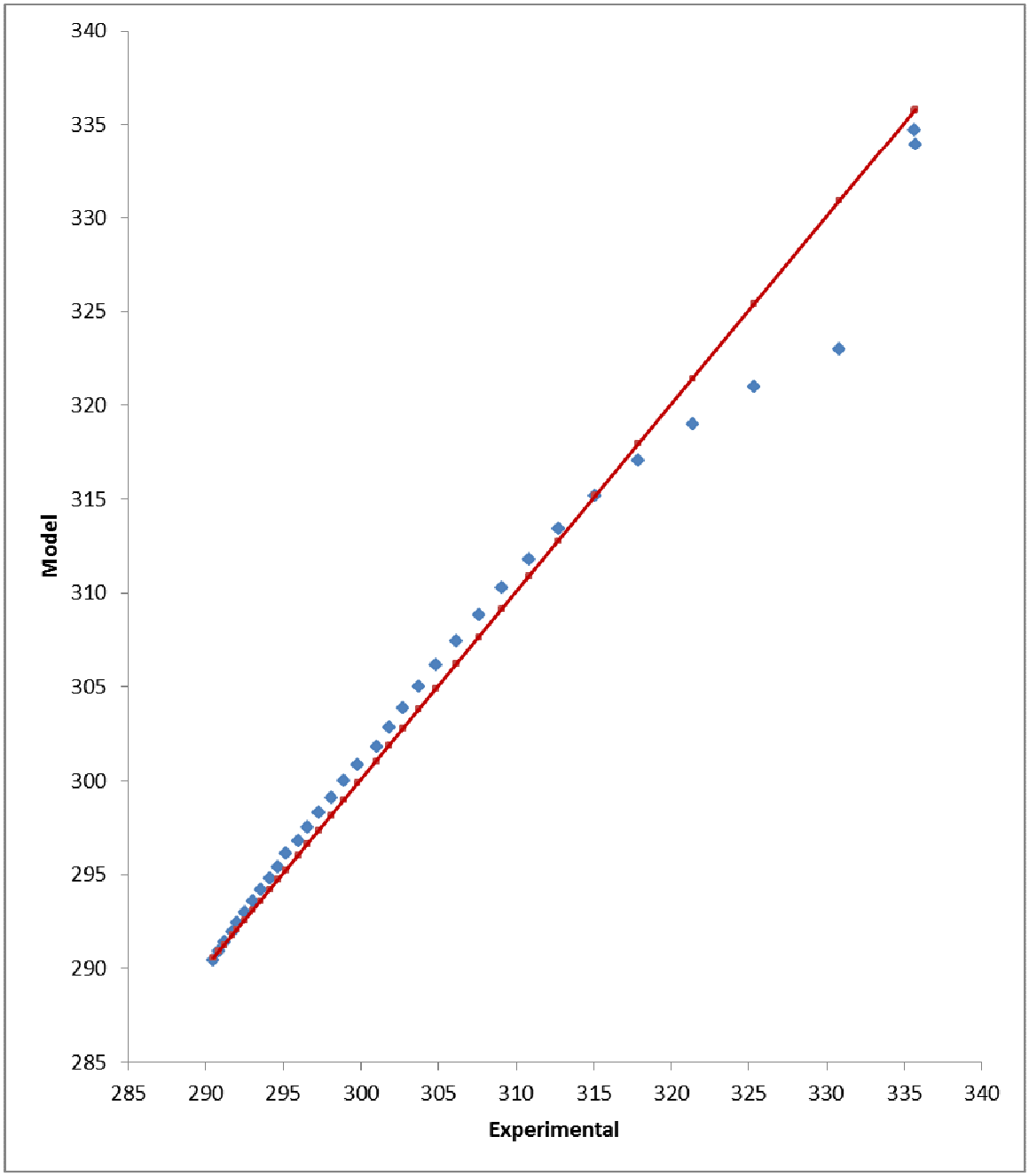

Figure (24b): Methya acetate parity plot of experiment (1):

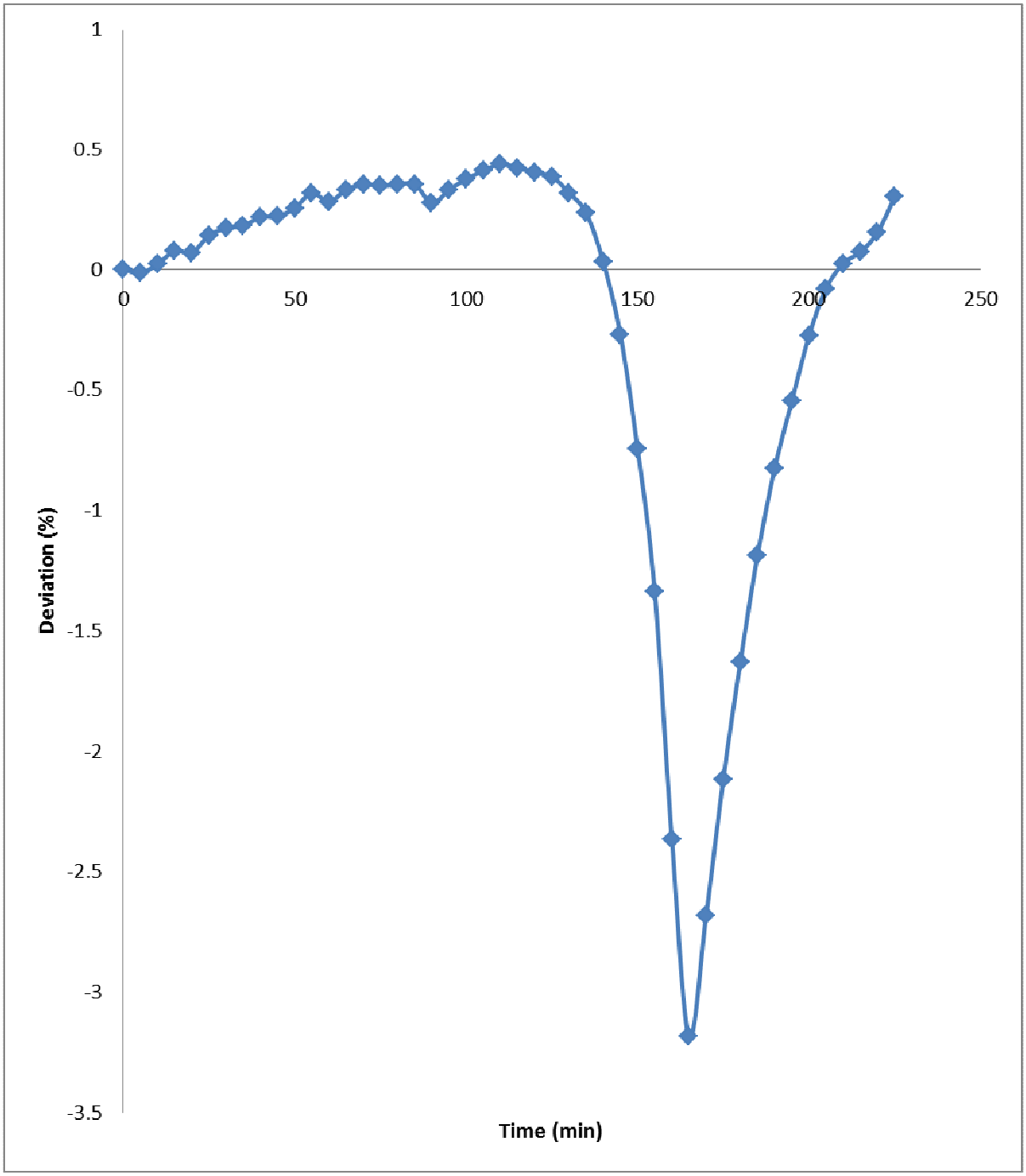

Figure (24c): Variation of model-predicted temperature with its associated deviation from experimental results-Experiment (1)

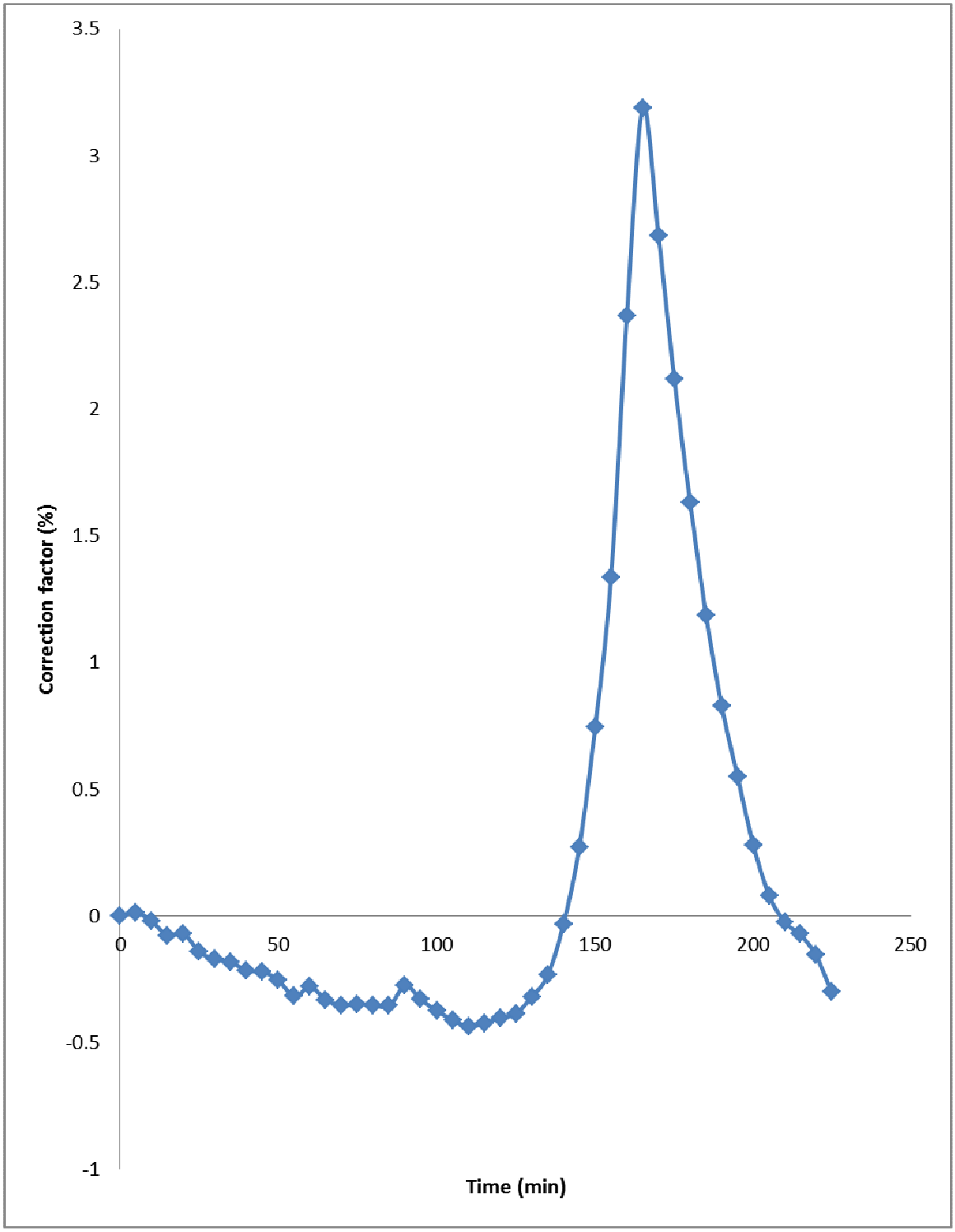

Figure (24d): Variation of model-predicted temperature with its associated correction factor-Experiment (1)

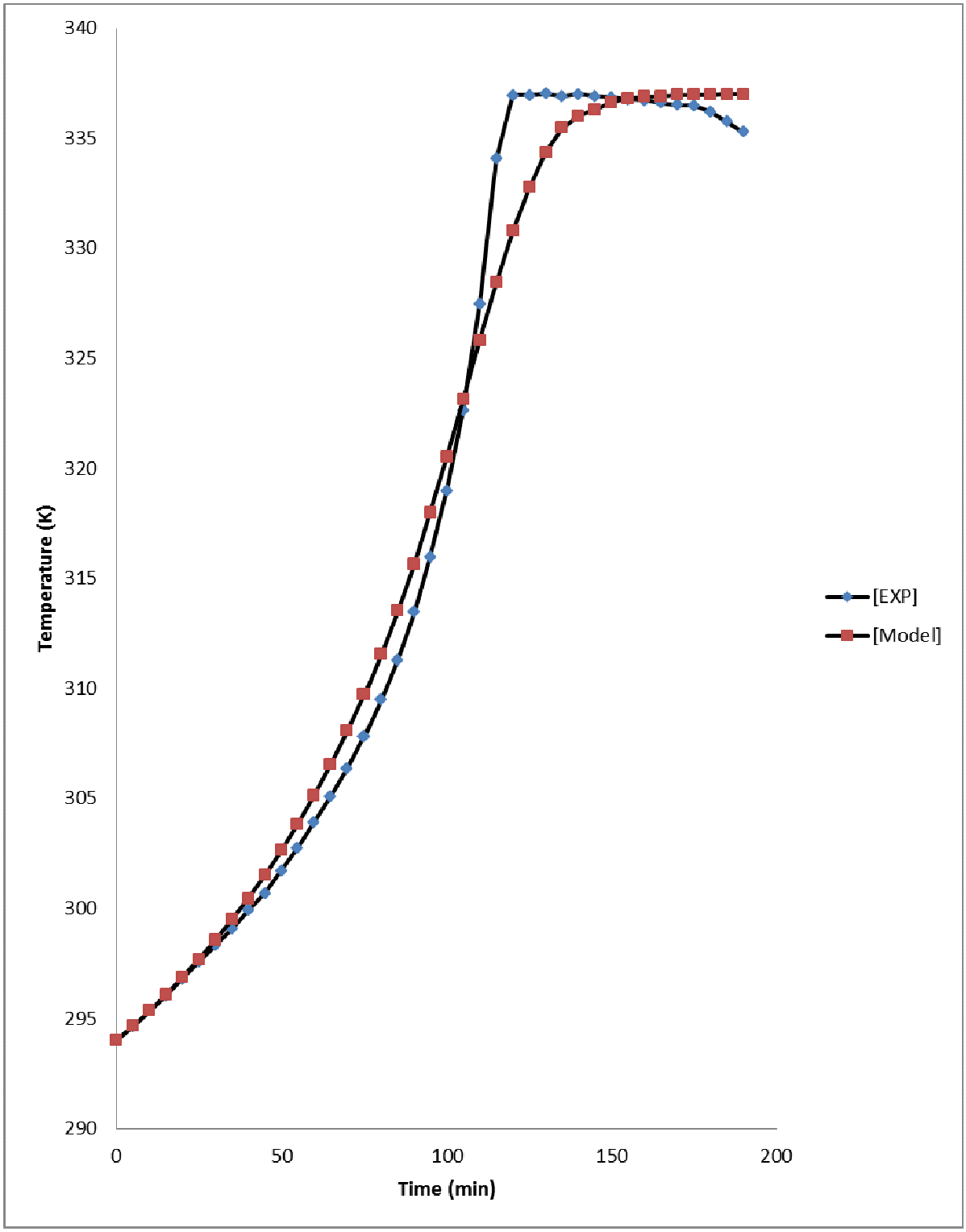

Figure (25a): Comparison of the model- predicted and experimentally measured temperature against time for experiment (2)

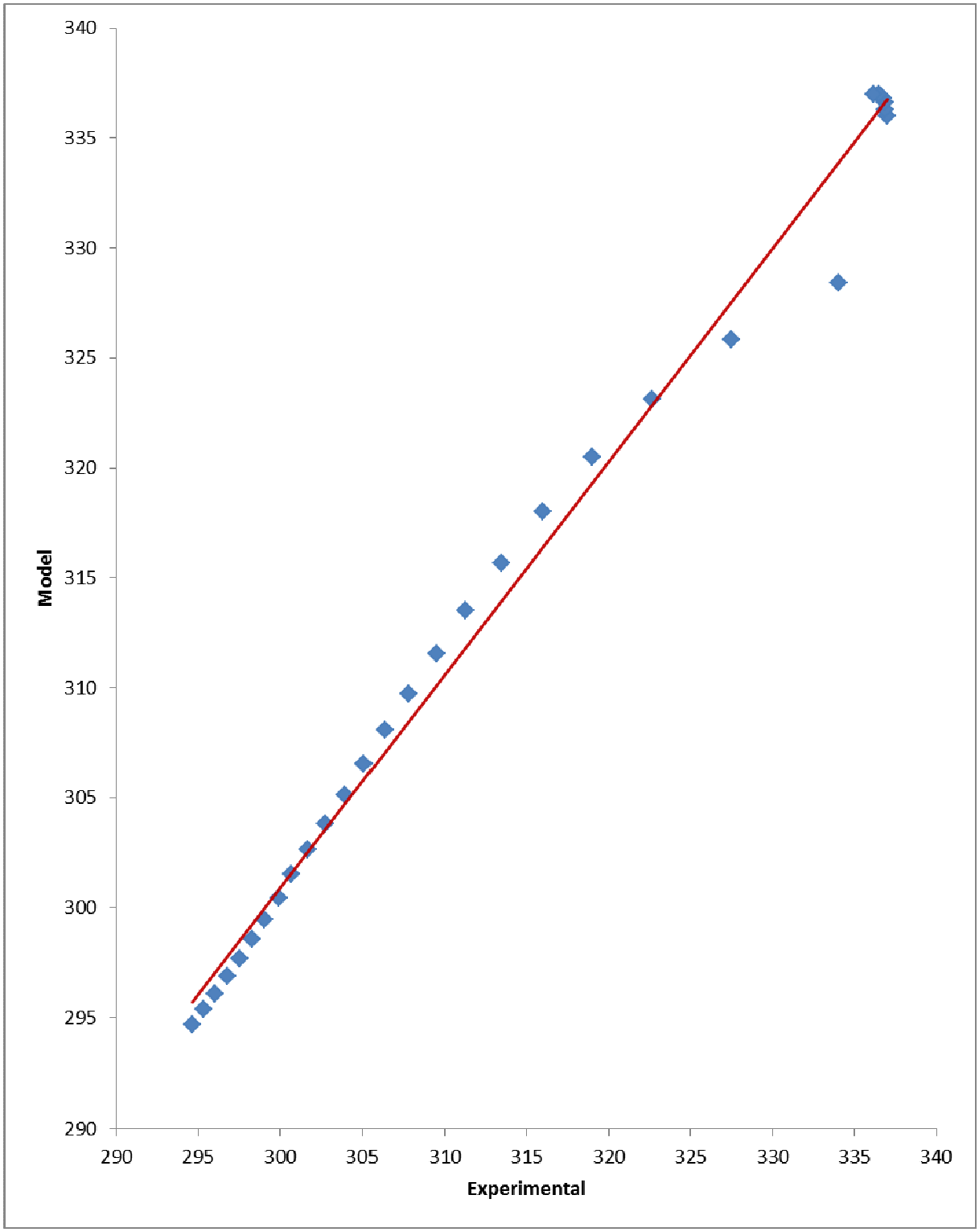

Figure (25b) show the parity plot of model-predicted and experimentally measured temperature of experiment (2):

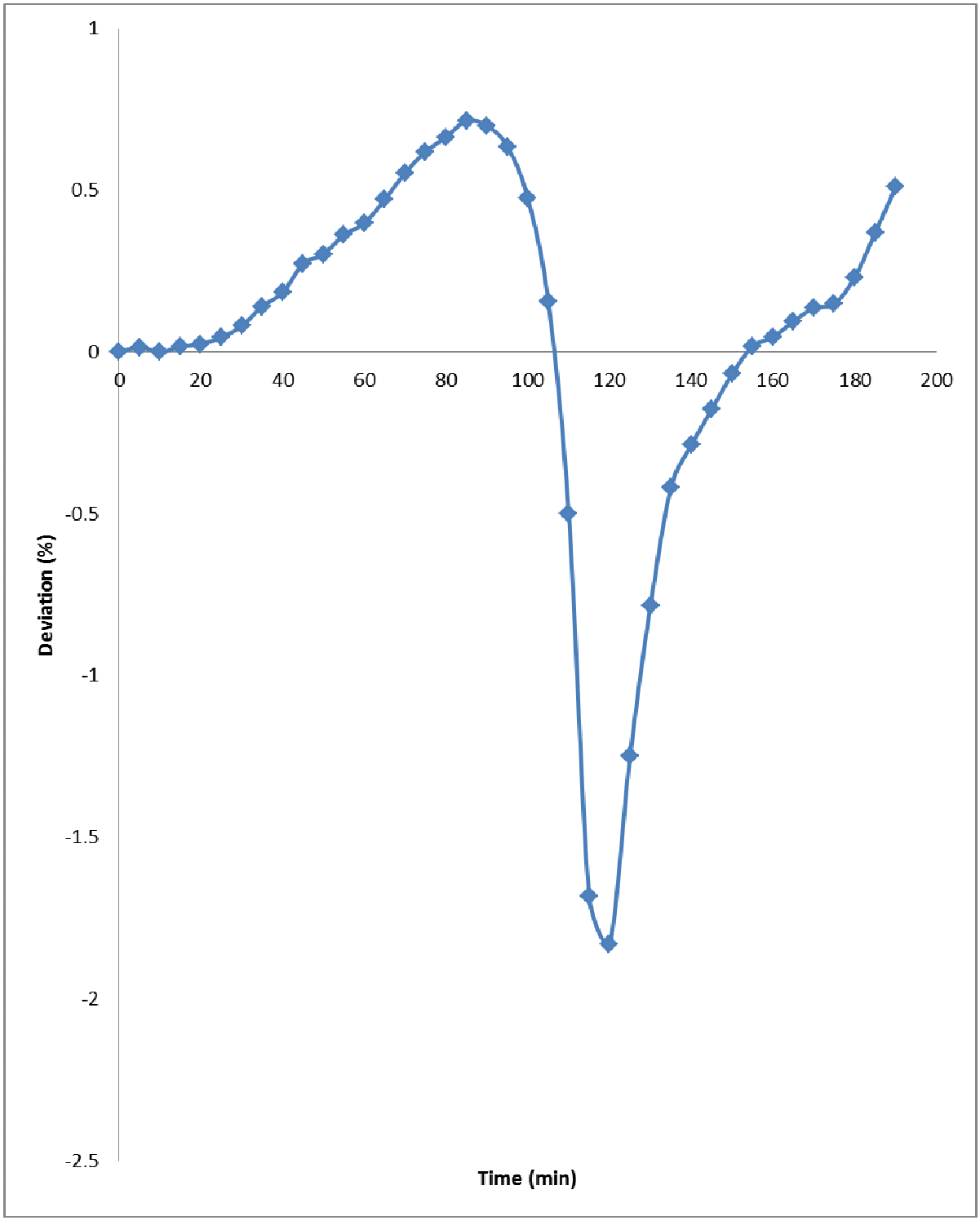

Figure (25c): Variation of model-predicted temperature with its associated deviation from experimental results-Experiment (2)

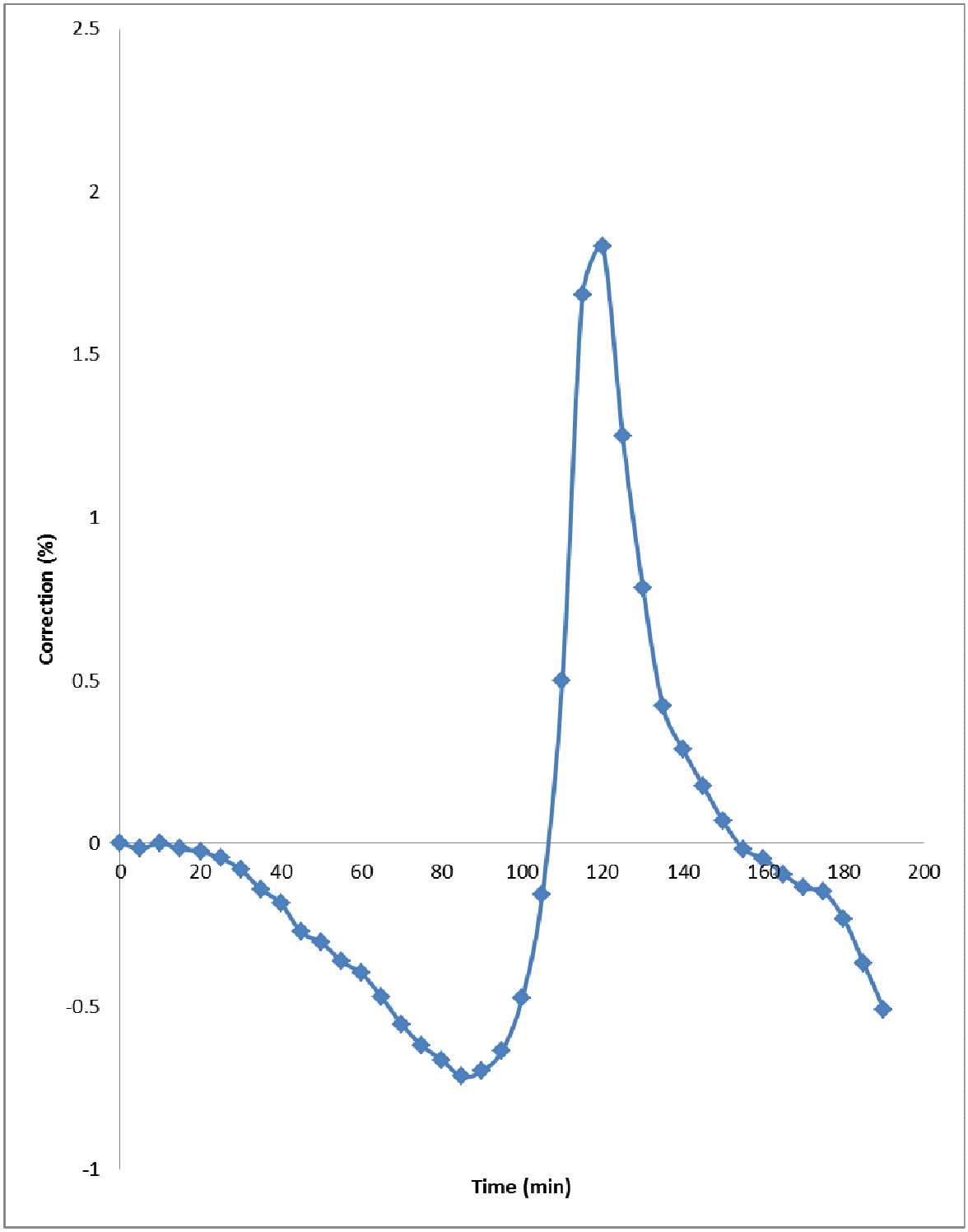

Figure (25d): Variation of model-predicted temperature with its associated correction factor-Experiment (2)

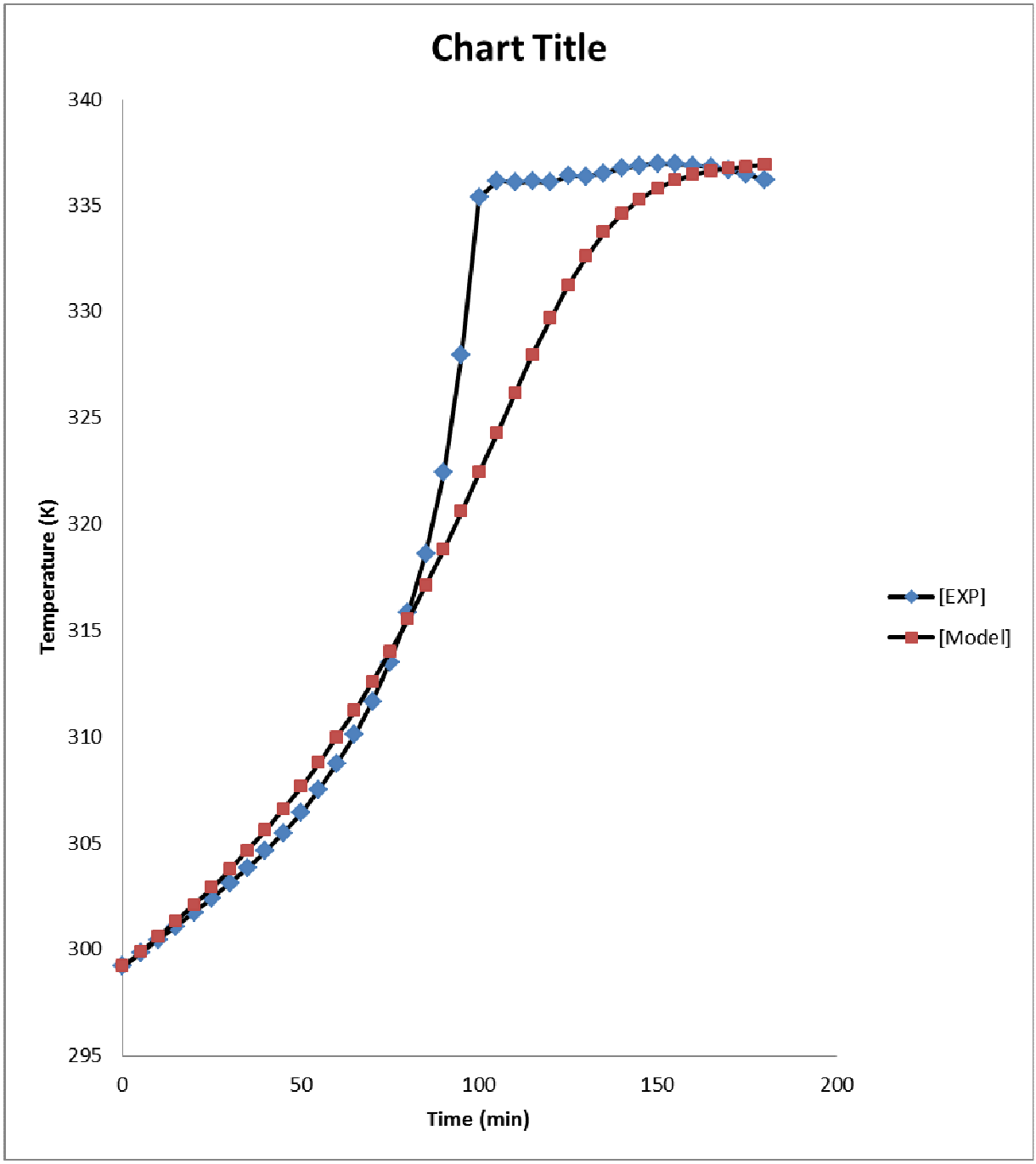

Figure (26a): Comparison of the model- predicted and experimentally measured temperature against time for experiment (3)

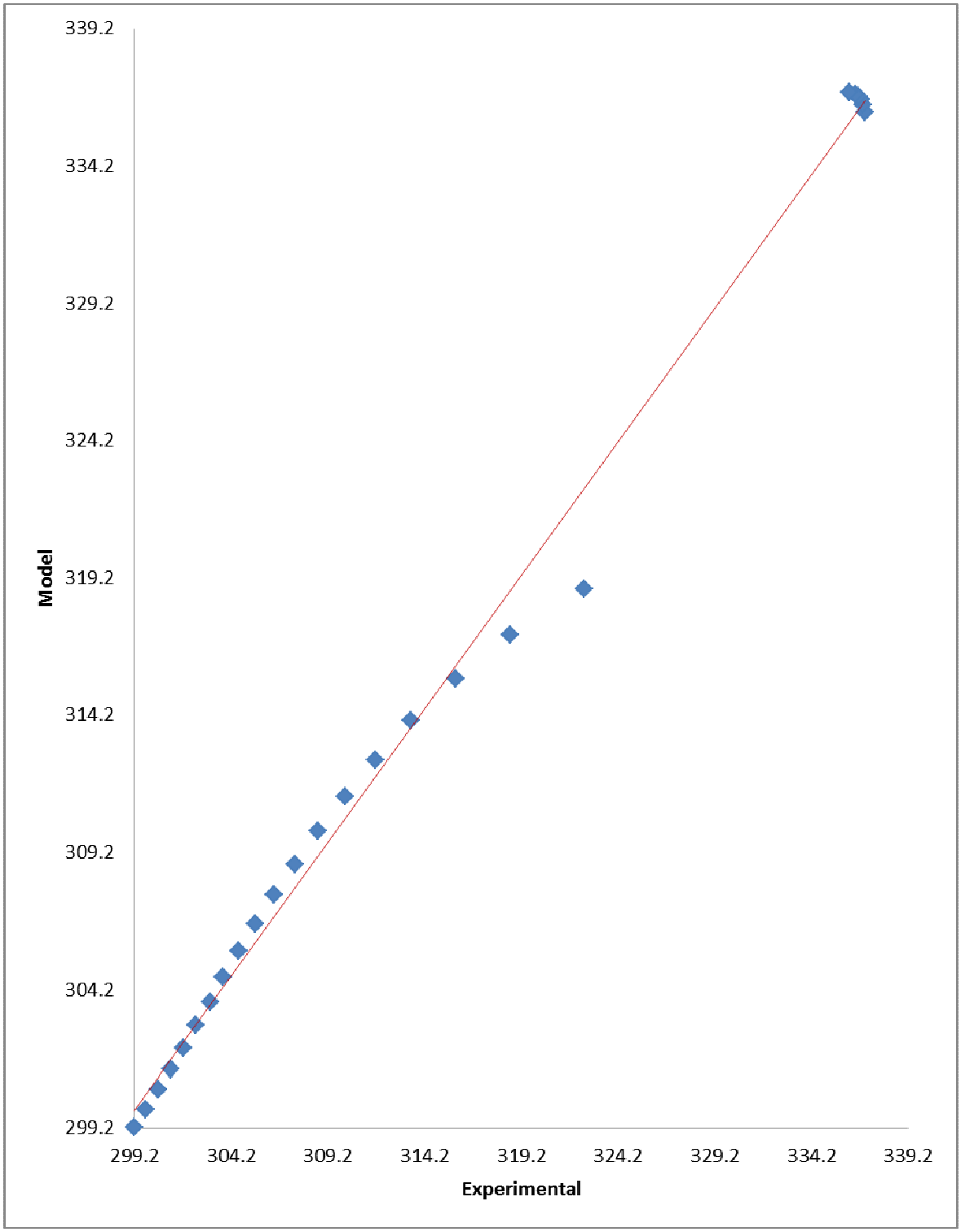

Figure (26b) show the parity plot of model-predicted and experimentally measured temperature of experiment (3)

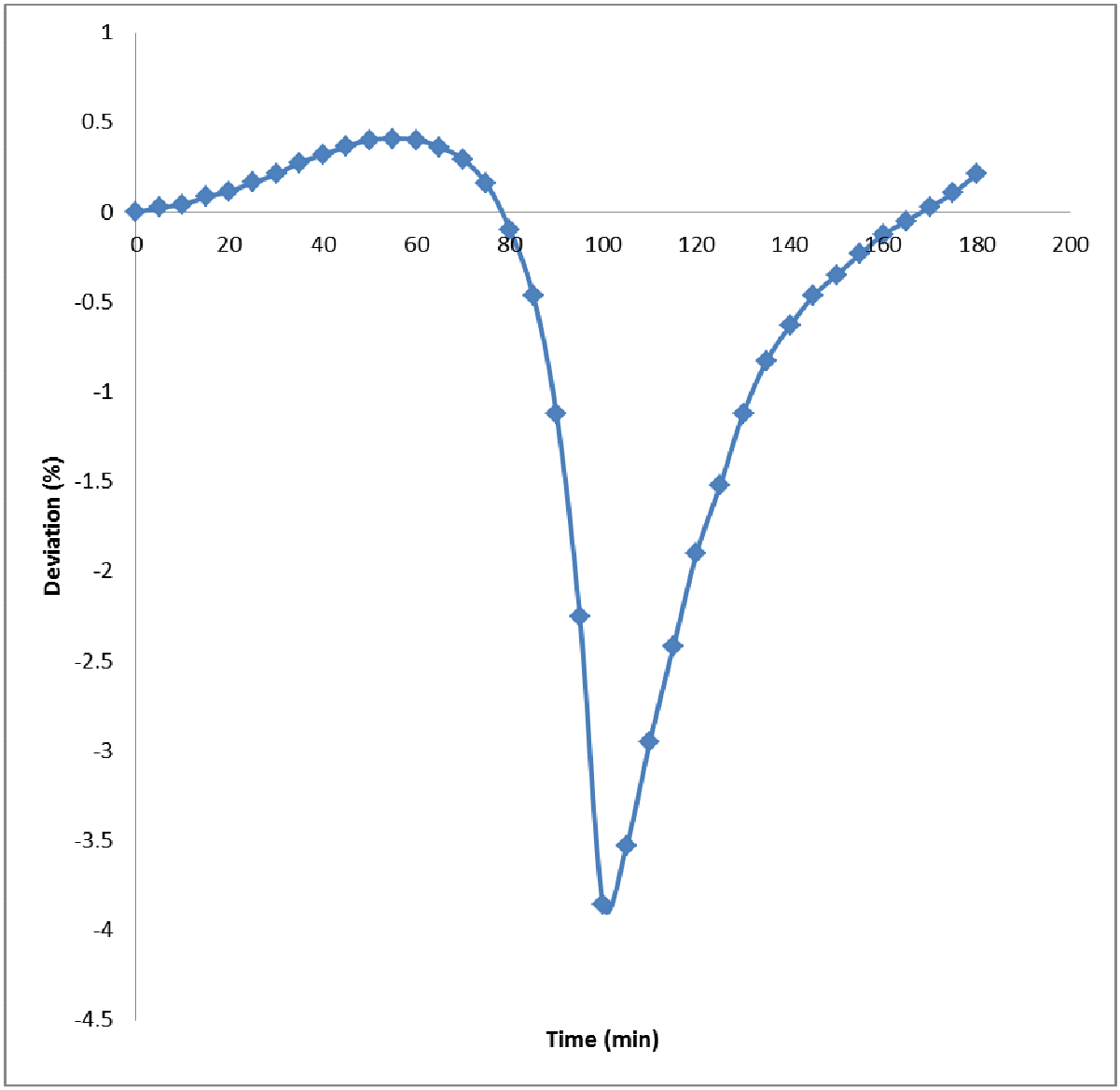

Figure (26c): Variation of model-predicted temperature with its associated deviation from experimental results-Experiment (3)

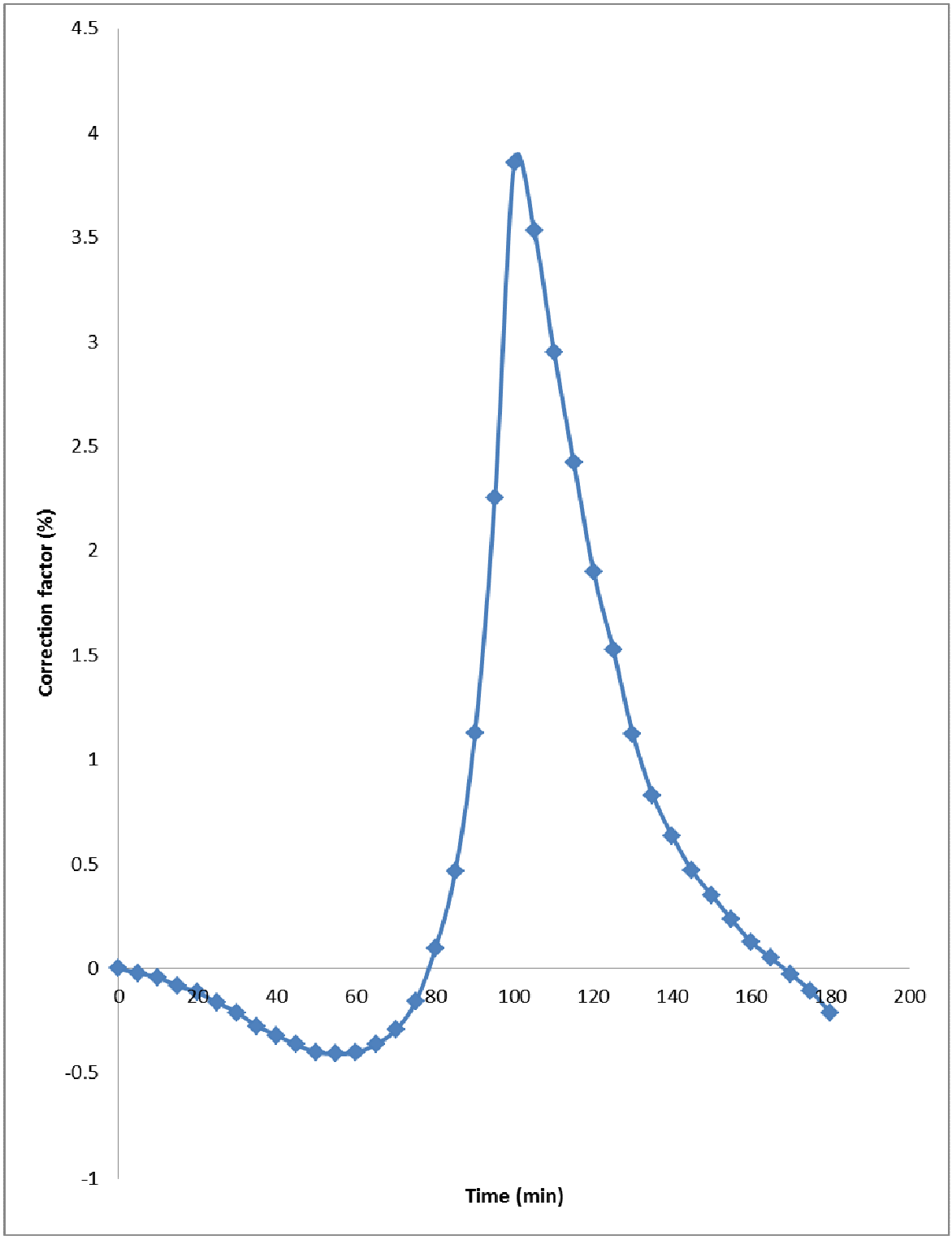

Figure (26d): Variation of model-predicted temperature with its associated correction factor-Experiment (3)

DISCUSSIONS

By direct comparison of model-predicted temperature profiles and experimentally measure temperature profiles it is seen if figures 24a, 25a and 26a the model proposed agree quite well in predicting the experimentally measure temperatures. The parity plots shown in figures 24b, 25b and 26c are also used as a means of validation of the proposed model. It is seen from the plots that there is good agreement between model-predicted temperatures and experimentally measured temperatures. An ideal comparison testing validity of the model is

achieved by considering the r-squared values (coefficient of determination). Comparing the data from both the model and the experiment it was noticed that the r-squared values were 0.980,0.991 and 0.994 respectively for experiments 1, 2 and 3. This suggest proximate agreement between model-predicted temperatures and that of the experimentally measure temperatures. The maximum percentage deviations of the model-predicted temperatures, from the corresponding experimental values are 3.18%, 1.83% and 3.86% for experiments 1, 2 and 3. The deviations are depicted graphically in figures 24c, 25c and 26c. The deviation values are quite within the acceptable deviation range of experimental results and give an indication of the reliability the usefulness of the proposed model. The correction factors which were the negative form of the deviations are shown in figures 24d, 25d and 26d. The correction factors take care of the effects of all the issues that were not considered during the experiments and the assumptions which were not catered for during the model formulation. The model as it stands can be used to predict liquid- phase temperature of the esterification process of acetic anhydride and methanol. The predicted temperatures can then be used to predict the liquid phase composition with the help of equation (9) above during reactive distillation process until the reaction reaches the maximum steady boiling temperature of 335K. At this near boiling temperature one expects the vapor-phase of the system to consist of some reactants and products species and by thermodynamic considerations the vapor-phase compositions can be predicted. This then constitute a step toward the preliminary design of reactive distillation system of the esterification process of acetic anhydride with methanol.

CONCLUSIONS

The mathematical models developed have shown satisfactory results in simulating the liquid-phase temperatures of the esterification of acetic anhydride with methanol. The results were found in good agreement with experimental results. The maximum deviation of the model-predicted temperatures was found to be not more than 4% in all cases which is quiet within acceptable range of experimental results. Nonetheless, further work should incorporate more process parameters into the model with the aim of reducing the deviations of the model-predicted temperature values from those of the experimentally measured observed values. The findings from the simulation results can be used to develop the technology (reactive distillation) to convert acetic anhydride-methanol system to methyl acetate and acetic acid.

LIST OF SYMBOLS

ΔH_{rxn}-heat of reaction (KJ/mol)
H-Enthalpy
H_o- Initial Enthalpy
ΔT (ad) –adiabatic temperature change (K)
$\Delta\varepsilon$ –extent of reaction
A –preexponential factor
B,C – thermistor constants
C_A-concentration of A (mol/L)
C_P –specific heat capacity
$C_{P,AA}$ –specific heat capacity of acetic anhydride
$C_{P,m}$ –specific heat capacity of methanol
$C_{P,mix}$-constant heat capacity of reaction mixture (kJ/mol.K)
$C_{P,W}$ –specific heat capacity of water
E_a – activation energy
I_{total} – total current of the circuit
K^o_{eqm} –Equilibrium constant
m –mass
M_{AA} –Mass of acetic anhydride
M_m –Mass of methanol
M_{eqv} –Equivalent amount of water
M_T-mass of reaction mixture(Kg)
N_A –mole of A (mol)
Q-heat produced by stirrer
R – molar gas constant
R_2 – known resistance in the circuit
$-r_A$ –rate of reaction of (A)
R_{TH} – Thermistor resistance
t – time
T_{amb} –ambient temperature

T_{max} –maximum temperature (K)
T_o –initial temperature
T-reactor temperature (K)
T_S – steady state temperature (K)
U –heat transfer coefficient (J/m^2 s.K)
v – total voltage of the circuit
V-Volume of vessel
V_{out} – voltage measured by thermistor
V_{TH} – voltage across thermistor resistance
X- conversion
β- constant

REFERENCES

Agreda, V. H., Partin, L. R., Heise, L. R., (**1990**), "High-Purity Methyl Acetate via Reactive Distillation", Chem. Eng. Prog. Vol 86 No.2, 40-46.

Bock, H., Jimoh, M., Wozny, G. (**1997)**, "Analysis of Reactive Distillation using the Esterification of Acetic Acid as an example", Chem. Eng. Technol. 20 182 -191.

Kenig, E. Y., Bäder, H., Górak, A., Beβling, B., Adrian, T., Schoenmakers, H., (**2001**),"Investigation of Ethyl Acetate Reactive Distillation Process", Chem. Eng. Sci.",6185 -6193.

Keys, D. B., (**1932**), " Esterification Processes and Equipment", Ind. Eng. Chem., Vol. 24, 1096 -1103.

Kreul, U. L., Gorak, A., Dittrich, C., (**1998**), "Catalytic Distillation: Advanced Simulation and Experimental Validation", Comp. Chem. Eng. Vol 22, 371 -373

Mohl, K, D., Kienle, A., Gilles, E. D., Rapmund, P., Sundmacher, K., Hoffmann, U. (**1997**), "Nonlinear Dynamics of Reactive Distillation Processes for the Production of Fuel Ether", Comp. Chem. Eng. Vol 21, S983-S994.

Popken, T., Steinigeweg, S., Gmehling, J., (**2001**), "Synthesis and Hydrolysis of Methyl Acetate Reactive Distillation using Structured Catalytic Packing: Experiments ans Simulation", Ind. Eng. Chem. Res., Vol. 40, 1566 -1574.

Teo, H. T. R., Saha, B., (**2004**)," Heterogeneous Catalysed Esterification of Acetic Acid with Isoamyl Alcohol: Kinetic Studied", J. Catal. 228 174 -182.